Article

Not peer-reviewed version

Spectroscopic Investigation of Losartan and Glipizide Competitive Binding to Glycated Albumin in Polypharmacotherapy: A Comparative Study

Agnieszka Szkudlarek *

Posted Date: 5 August 2024

doi: 10.20944/preprints202408.0250.v1

Keywords: polypharmacotherapy; spectroscopic investigation; losartan; glipizide; glycated albumin; diabetes; AGEs; drug-albumin binding; drug-drug interactions

Article

Spectroscopic Investigation of Losartan and Glipizide Competitive Binding to Glycated Albumin in Polypharmacotherapy: A Comparative Study

Agnieszka Szkudlarek *

Department of Physical Pharmacy, Faculty of Pharmaceutical Sciences in Sosnowiec, Medical University of Silesia in Katowice, 40-055 Katowice, Poland; aszkudlarek@sum.edu.pl; Tel.: +48-32-364-1597

Abstract: Understanding the interaction between pharmaceuticals and serum proteins is crucial for optimizing therapeutic strategies, especially in patients with coexisting chronic diseases. The primary goal of this study was to assess the potential changes in binding affinity and competition between glipizide (GLP, a second-generation sulfonylurea hypoglycemic drug) and losartan (LOS, a medication commonly prescribed for hypertension, particularly for patients with concurrent diabetes) with non-glycated (HSA) and glycated ($gHSA_{GLC}$, $gHSA_{FRC}$) human serum albumin using multiple spectroscopic techniques (fluorescence, UV-visible absorption, and circular dichroism spectroscopy). The results indicate that FRC is a more effective glycation agent for HSA than GLC, significantly altering the albumin structure and affecting the microenvironment around critical amino acid residues, Trp-214 and Tyr. These modifications reduce the binding affinity of LOS and GLP to $gHSA_{GLC}$ and $gHSA_{FRC}$, compared to HSA, resulting in less stable drug-protein complexes. The study reveals that LOS and GLP interact nonspecifically with the hydrophobic regions of the albumin surface in both binary (ligand-albumin) and ternary systems (ligand-albumin-$ligand_{const}$) and specifically saturate the binding sites within the protein molecule. Furthermore, the presence of an additional drug (GLP in the LOS-albumin complex or LOS in the GLP-albumin complex) complicates the interactions, likely leading to competitive binding or displacement of the initially bound drug in both non-glycated and glycated albumins. Analysis of the CD spectra suggests mutual interactions between GLP and LOS, underscoring the importance of closely monitoring patients co-administered these drugs to ensure optimal therapeutic efficacy and safety.

Keywords: polypharmacotherapy; spectroscopic investigation; losartan; glipizide; glycated albumin; diabetes; AGEs; drug-albumin binding; drug-drug interactions

1. Introduction

The escalating prevalence of chronic diseases, including hypertension and type 2 diabetes mellitus, has necessitated the widespread use of polypharmacotherapy. This therapeutic approach mandates a comprehensive understanding of drug interactions and their biochemical implications, mainly when pharmaceuticals interact with modified biological molecules such as glycated human serum albumin (gHSA). gHSA, a product of non-enzymatic glycation of human serum albumin (HSA), is prevalent in diabetic patients and has significant clinical implications due to its altered structure, biological function, and physicochemical properties [1,2].

Albumin, the primary protein in human plasma, is essential for maintaining oncotic pressure and transporting various endogenous and exogenous substances. Furthermore, HSA possesses anti-inflammatory, antioxidant, and antithrombotic properties [3]. Under diabetic conditions, HSA undergoes glycation, which can markedly affect its drug-binding capabilities. Glycated albumin serves not only as a marker of short-term glycemic control but also influences the pharmacokinetics and pharmacodynamics of therapeutic agents, potentially altering their efficacy and safety profiles [4]. Understanding how glycation modifies albumin's binding properties is essential for optimizing drug dosing and minimizing adverse effects in diabetic patients.

 doi:10.20944/preprints202408.0250.v1

Losartan (LOS, Figure 1a) is widely used for its antihypertensive properties, primarily by inhibiting the renin-angiotensin system. By blocking angiotensin II from binding to the AT1 receptor, LOS induces vasodilation and decreases aldosterone secretion, lowering blood pressure [5,6]. LOS exhibits a high affinity to HSA, predominantly binding at site II, also known as the benzodiazepine-binding site [7]. This significant binding within subdomain IIIA of the HSA macromolecule ensures that a considerable portion of LOS remains inactive in the bloodstream, with only a minor fraction available as a free drug to exert its therapeutic effects.

Glipizide (GLP, Figure 1b), a second-generation sulfonylurea, is widely used to manage blood glucose levels in patients with type 2 diabetes mellitus. It exerts its pharmacological effects by stimulating insulin secretion from pancreatic β-cells. This is achieved by inhibiting ATP-sensitive potassium channels on the β-cell membrane, leading to membrane depolarization and subsequent insulin release, thereby reducing blood glucose levels [8]. The study using high-performance affinity chromatography (HPAC) revealed that GLP interacts with both Sudlow's sites I and II on HSA but with greater affinity for site II than the site I [9]. Anwer et al. performed molecular docking and simulation studies in silico, showing that the glipizide-HSA complex is formed due to hydrogen bonds and hydrophobic interactions [8].

In combination therapy, LOS and GLP may compete for the same binding site on HSA. This competitive binding can influence their pharmacokinetics and pharmacodynamics, potentially affecting their efficacy and safety profiles. The primary aim of this study was to compare the interactions of losartan and glipizide with human serum albumin– both non-glycated (HSA) and glycated by glucose (gHSA$_{GLC}$) and fructose (gHSA$_{FRC}$)– and to investigate their mutual binding interactions using spectroscopic techniques (fluorescence spectroscopy, UV-visible absorption spectroscopy, and circular dichroism spectroscopy – CD). These techniques are widely recognized for studying in vitro interactions of drugs with albumin due to their sensitivity, speed, and simplicity [10–12]. They are beneficial for calculating binding and quenching parameters, mean residue ellipticity, and characterizing proteins' secondary and tertiary structures.

By elucidating the competitive binding interactions of LOS and GLP with glycated albumin at a molecular level, this research seeks to provide insights that could inform better clinical practices in polypharmacotherapy, particularly for patients at risk of altered drug efficacy due to glycation. This understanding is imperative for optimizing therapeutic strategies in patients with comorbid hypertension and diabetes.

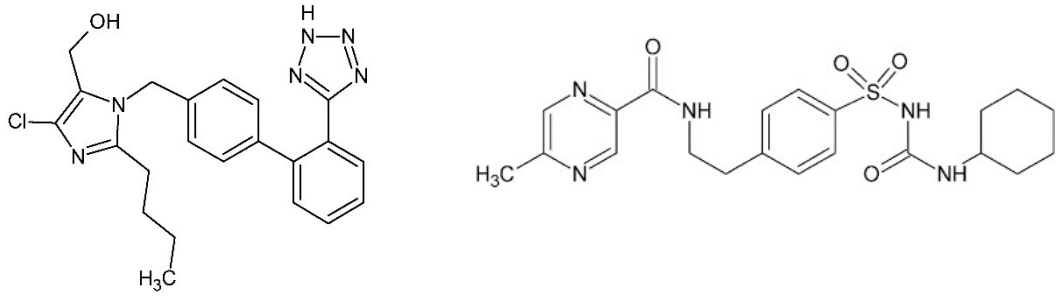

(**a**) (**b**)

Figure 1. Chemical structure of (**a**) losartan (LOS) and (**b**) glipizide (GLP). The structural formulas of LOS and GLP were rendered using the ChemSketch ver. 12.1.0.31258 program.

2. Results and Discussion

2.1. HSA Glycation – Formation of Glycation Products

Reducing sugars, such as glucose (GLC) and fructose (FRC), react with the primary free amino groups of the NH_2-terminal amino acid and/or the ε-amino group of lysine (Lys), arginine (Arg), and the thiol group of cysteine (Cys-34), leading to their glycation. The final stage of this process is the formation of AGEs – Advanced Glycation End-products, a heterogeneous group of compounds

 doi:10.20944/preprints202408.0250.v1

considered a critical pathophysiological factor in diabetic complications [13]. In vitro studies utilize various glycation agents and specific experimental conditions to initiate the glycation process. GLC, the most abundant sugar in the human body, plays a critical role in the endogenous formation of AGEs and serves as an essential biomarker in the assessment of diabetes. However, recent research has demonstrated that diabetes is also associated with abnormal fructose metabolism. Uric acid, produced from endogenous fructose, can lead to kidney and cardiovascular disease, hypertension, and obesity in diabetic patients, as FRC is generated via the polyol pathway [14,15]. Accordingly, glucose, the body's primary energy source, and fructose, a dietary reducing sugar, were prompted to be used as glycation agents for human serum albumin (HSA) under in vitro conditions.

A comparative analysis of the emission fluorescence spectra of glycation products formed in glycated albumin (gHSA$_{GLC}$, gHSA$_{FRC}$) and those present in non-modified HSA showed a significant increase in the fluorescence intensity of AGEs in the glycated proteins upon excitation at λ_{ex} = 335 nm (Figure 2a) and λ_{ex} = 485 nm (Figure 2b).

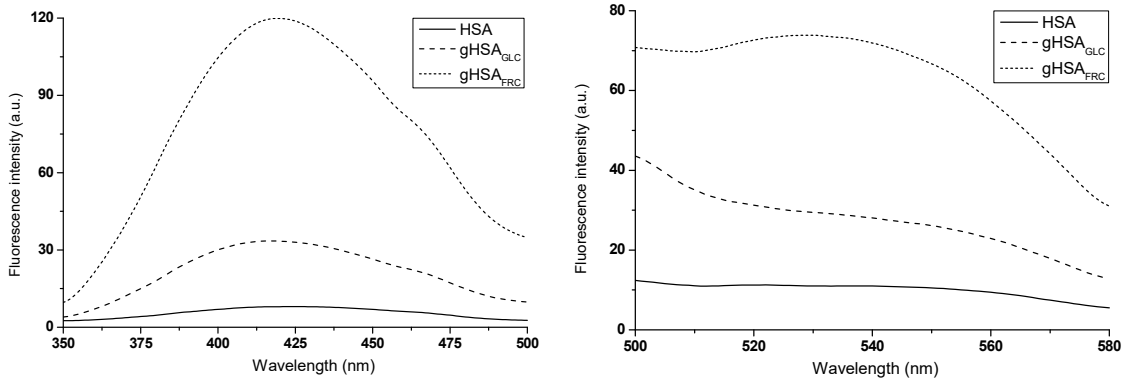

Figure 2. Emission fluorescence spectra of AGEs present in HSA and formed in gHSA$_{GLC}$ and gHSA$_{FRC}$ excited at (**a**) λ_{ex} = 335 nm and (**b**) λ_{ex} = 485 nm; protein concentration is 5 × 10^{-6} mol·L^{-1}.

From the experiment results, it is evident that FRC induces glycation of HSA more effectively than GLC. The higher fluorescence intensity of AGEs observed in gHSA$_{FRC}$ suggests that HSA undergoes a faster and more efficient Amadori rearrangement in the presence of FRC than in the HSA-GLC system. In addition to the hyperchromic effect, this study observed a hypsochromic shift of the fluorescence maxima of glycated albumin AGEs compared to HSA excited at λ_{ex} = 335 nm ($\Delta\lambda_{max}$ = 6 nm). This blue shift indicates a decrease in polarity within the environment of the newly formed products (Figure 2a). Irradiation in the wavelength ranges of 320 nm to 335 nm and 325 nm to 335 nm causes the excitation of argpyrimidine (AP) and pentosidine (PEN), respectively. These compounds, which exhibit fluorescent properties, are formed due to protein modifications by methylglyoxal through interactions with arginine residues in macromolecules [16]. AP emits fluorescence at an approximate wavelength of λ_{em} ~ 400 nm, while PEN in the range of λ_{em} = 375 nm to 385 nm [17]. The glycated albumin products gHSA$_{GLC}$ and gHSA$_{FRC}$, when excited at λ_{ex} = 335 nm (Figure 2a), do not display fluorescence typical of PEN and AP. The fluorescence of AGEs at around λ_{em} = 420 nm suggests the formation of PEN and AP in glycated proteins but also indicates the presence of additional fluorophores. This is evidenced by the shift of the fluorescence maximum towards longer wavelengths compared to the emission of PEN and AP, as described by Kessel et al. [17]. An advantage of measurements at λ_{ex} = 485 nm is the absence of interference from other fluorophores in the sample. According to Schmitt et al., fluorescence with an emission maximum at λ_{em} = 530 nm (Figure 2b) appears to be an indicator of arginyl residue modifications [18]. The results presented here confirm the efficacy of the glycation process under the experimental conditions applied in this study, providing a solid foundation for further research in this area.

 doi:10.20944/preprints202408.0250.v1

2.2. Investigating the Interaction of Losartan and Glipizide with Non-Glycated and Glycated Human Serum Albumin in Binary and Ternary Complexes

Assessing changes in the fluorescence emission intensities of aromatic amino acid residues within proteins can effectively reveal intermolecular interactions [19]. Human serum albumin (HSA) contains 18 fluorescent tyrosine residues (Tyr-9, Tyr-39, Tyr-84, Tyr-138, Tyr-140, Tyr-148, Tyr-150, Tyr-161, Tyr-263, Tyr-319, Tyr-332, Tyr-334, Tyr-340, Tyr-341, Tyr-372, Tyr-375, Tyr-401, Tyr-411), along with a single, strongly fluorescent tryptophan residue (Trp-214) buried within a hydrophobic pocket [20]. The fluorescence quenching technique is commonly employed to determine the strength and mechanism of interactions between ligands (drugs) and albumin, especially involving the Trp-214 and Tyr residues located within albumin's subdomains IIA and/or IB, IIB, and IIIA.

Fluorescence quenching of non-glycated (HSA) and glycated (gHSA$_{GLC}$, gHSA$_{FRC}$) albumin, excited at λ_{ex} = 275 nm and λ_{ex} = 295 nm, was performed to determine the interaction of losartan (LOS) and glipizide (GLP) at high-affinity binding sites of albumins in the binary systems: LOS-HSA (Figure 3a), LOS-gHSA$_{GLC}$ (Figure 3b), LOS-gHSA$_{FRC}$ (Figure 3c), GLP-HSA (Figure 3d), GLP-gHSA$_{GLC}$ (Figure 3e), GLP-gHSA$_{FRC}$ (Figure 3f).

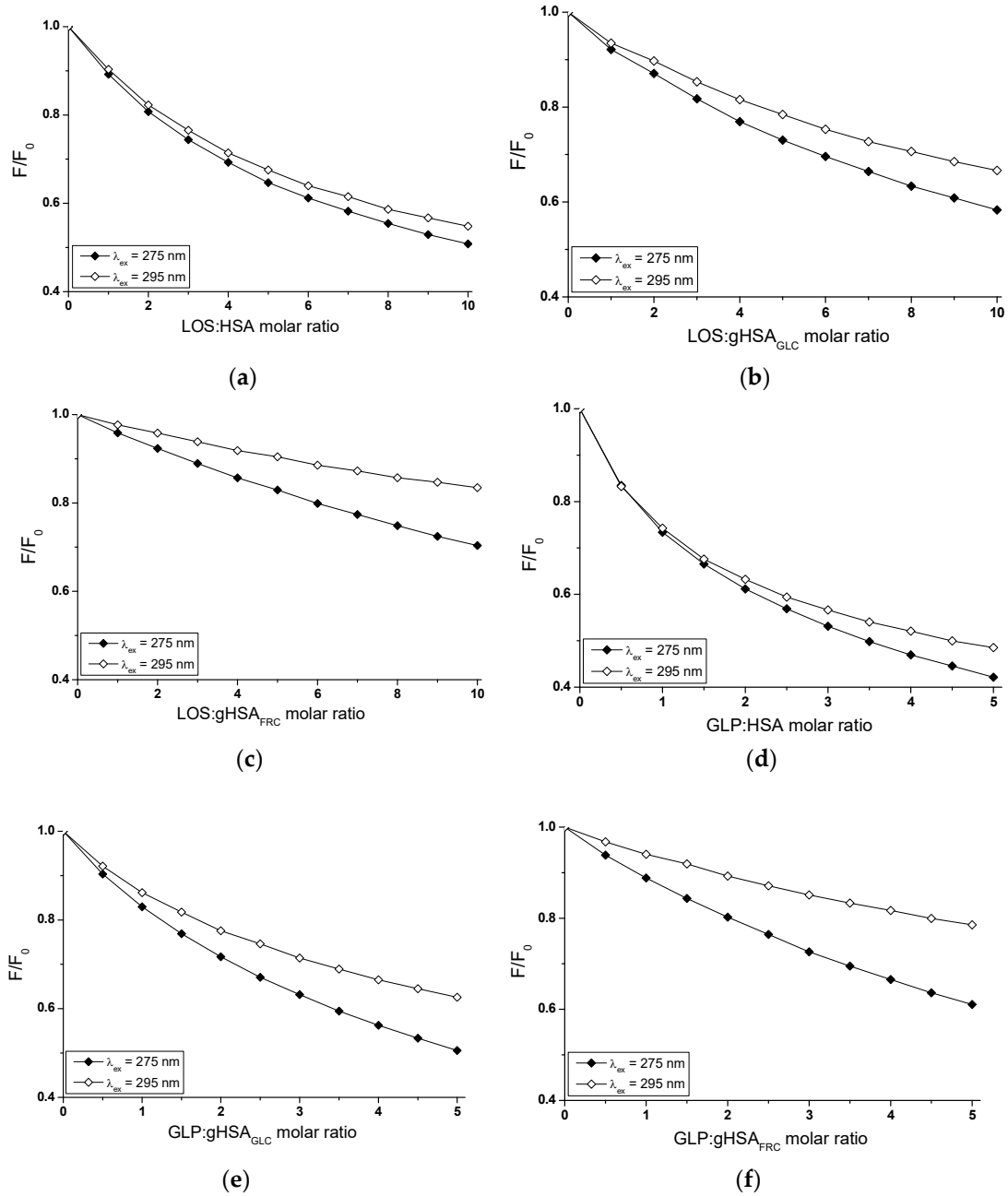

 doi:10.20944/preprints202408.0250.v1

Figure 3. Quenching fluorescence of HSA (**a**, **d**), gHSA$_{GLC}$ (**b**, **e**) and gHSA$_{FRC}$ (**c**, **f**) containing 5 × 10^{-6} mol·L^{-1} to 5 × 10^{-5} mol·L^{-1} concentrations of LOS (**a–c**) and 2.5 × 10^{-6} mol·L^{-1} to 2.5 × 10^{-5} mol·L^{-1} concentrations of GLP (**d–f**). Albumin concentration: 5 × 10^{-6} mol·L^{-1}; λ_{ex} = 275 nm (♦) and λ_{ex} = 295 nm (◊); error bars are smaller than the symbols.

In fluorescence studies, attention is directed towards specific protein regions containing fluorophores. Using an excitation wavelength of 275 nm enables the observation of both tryptophan (Trp-214) and tyrosine (Tyr) residues, whereas a 295 nm wavelength selectively excites Trp-214 due to its unique spectral characteristics. The primary drug-binding sites are located within the IIA and IIIA subdomains of HSA. Both hydrophobic pockets contain at least one type of the mentioned amino acids, which can transfer energy to a ligand if it is close to the fluorophore [21].

In Sudlow's site I, located in the IIA subdomain, one tryptophan (Trp-214) and one tyrosine (Tyr-263) residue can participate in drug binding. Although Trp-214 is the sole tryptophan in the HSA structure, it plays a vital role in ligand interactions. The IIIA subdomain includes three tyrosine residues (Tyr-401, Tyr-411, and Tyr-497), which can transfer energy to the acceptor [22]. Additionally, Tyr-401 and Tyr-411 have been identified as amino acids that stabilize the binding of numerous ligands. To verify subdomain IIIA of human serum albumin as the specific binding site for LOS and GLP, quenching curves of HSA, gHSA$_{GLC}$ and gHSA$_{FRC}$ excited at λ_{ex} = 275 nm were compared with those excited at λ_{ex} = 295 nm with the addition of LOS (Figures 3a–c) and GLP (Figures 3d–f) at increasing concentrations.

As mentioned earlier, protein fluorescence quenching occurs when the distance between the chromophores in the aromatic rings of the ligand's chemical structure and the fluorophores of albumin is less than 10 nm according to Stryer [23] and less than 7 nm according to Valeur [21]. This proximity enables fluorescence resonance energy transfer (FRET) from a donor (fluorophore) to an acceptor (chromophore), leading to non-radiative, direct energy transfer to the drug molecule. The quenching curves of HSA (Figures 3a,d), gHSA$_{GLC}$ (Figures 3b,e) and gHSA$_{FRC}$ (Figures 3c,f) in the presence of both losartan and glipizide at increasing concentrations (with molar ratios of ligand to albumin from 1:1 to 10:1 for LOS and 1:1 to 5:1 for GLP) indicate a decrease in fluorescence for non-glycated and glycated albumin at excitation wavelengths of 275 nm and 295 nm. This indicates effective energy transfer between albumin fluorophores and the ligands. After applying corrections for the inner filter effect, the observed fluorescence quenching of HSA, gHSA$_{GLC}$, gHSA$_{FRC}$ can be attributed to the formation of LOS-HSA, LOS-gHSA$_{GLC}$, LOS-gHSA$_{FRC}$ and GLP-HSA, GLP-gHSA$_{GLC}$, GLP-gHSA$_{FRC}$ complexes.

Based on the data collected in Table S1 (Supplementary Materials), the percentage of non-glycated HSA fluorescence quenching, used as a control albumin, is nearly similar, reaching approximately 49.20% and 45.17% for LOS and 57.86% and 51.46% for GLP at λ_{ex} = 275 nm and λ_{ex} = 295 nm, respectively. For glycated albumin, weaker fluorescence quenching was observed in the presence of increasing ligand concentrations compared to the control sample, with the weakest quenching seen for albumin glycated by fructose (gHSA$_{FRC}$). LOS quenches the fluorescence of gHSA$_{GLC}$ by 41.67% at λ_{ex} = 275 nm and by 33.36% at λ_{ex} = 295 nm. The fluorescence of gHSA$_{FRC}$ decreases by 29.62% at 275 nm and by 16.54% at 295 nm for the same molar ratio of ligand to albumin (10:1). GLP quenches the fluorescence of gHSA$_{GLC}$ by 49.42% at λ_{ex} = 275 nm and by 37.41% at λ_{ex} = 295 nm, at molar ratio GLP:albumin 5:1. In contrast, the fluorescence of gHSA$_{FRC}$ at λ_{ex} = 275 nm and λ_{ex} = 295 nm decreases by 38.93% and 21.46%, respectively. Moreover, the data presented in Table S1 indicate that both LOS and GLP have a higher affinity towards non-glycated macromolecule than towards glycated proteins (gHSA$_{GLC}$ and gHSA$_{FRC}$).

The quenching curves of albumins excited at λ_{ex} = 275 nm and λ_{ex} = 295 nm in the presence of LOS (Figures 3a–c) and GLP (Figures 3d–f) at increasing drug concentration do not overlap above the molar ratio LOS:HSA 2:1, LOS:gHSA$_{GLC}$ 1:1, LOS:gHSA$_{FRC}$ 1:1 and GLP:HSA 1.5:1, GLP:gHSA$_{GLC}$ 0.5:1. The exact course of fluorescence quenchning curves indicates that there is no difference in energy transfer between the tyrosyl residues and the ligand, suggesting that initially only Trp-214 residue is likely involved in the interaction with LOS and GLP. This may allow the identification of subdomain IIA as a high-affinity binding site in the albumin structure. In contrast, a different

 doi:10.20944/preprints202408.0250.v1

trajectory of fluorescence quenching suggests that both tryptophanyl residue in subdomain IIA and tyrosyl residues located in hydrophobic subdomains IB, IIB, IIIA, and IIIB are involved in the interaction with LOS and GLP in the binding site environment. As shown in Figure 3, the fluorescence quenching of HSA (Figures 3a,d), gHSA$_{GLC}$ (Figures 3b,e), and gHSA$_{FRC}$ (Figures 3c,f) by LOS and GLP is more pronounced when excited at λ_{ex} = 275 nm compared to λ_{ex} = 295 nm. This likely indicates a significant involvement not only of Trp-214 but also of Tyr residues in the interaction between the ligands and albumins.

The quenching curves of non-glycated and glycated albumin in the presence of LOS (Figures S1ab, Supplementary Materials) and GLP (Figures S1cd, Supplementary Materials) exhibit significant differences in their profiles. Specifically, these differences result from 7.53% and 11.81%, 19.58% and 28.63% lower quenching of gHSA$_{GLC}$ and gHSA$_{FRC}$ by LOS relative to the LOS-HSA system at λ_{ex} = 275 nm and λ_{ex} = 295 nm, respectively. For the GLP-gHSA$_{GLC}$ and GLP-gHSA$_{FRC}$ systems, the differences in the quenching curves profiles amount to 8.44% and 14.05% for gHSA$_{GLC}$, and 18.93% and 30% for gHSA$_{FRC}$ relative to the GLP-HSA system at λ_{ex} = 275 nm and λ_{ex} = 295 nm, respectively (Table S1). Several factors may explain these observed differences. Glycation induces conformational changes in the albumin structure, modifying the binding sites and overall protein flexibility and affecting the interaction with quenchers. Additionally, glycation alters the microenvironment around crucial amino acid residues, such as Trp-214 and Tyr, influencing their accessibility to quenchers. The binding affinity of glycated albumin for LOS and GLP may also differ due to sugar moieties, which can either hinder or facilitate quencher binding [24]. Furthermore, steric hindrance from added sugar groups can reduce quenching efficiency, while new chemical interactions and potential protein aggregation further impact the quenching dynamics. These combined factors contribute to the distinct quenching behaviours observed for non-glycated and glycated albumin at different excitation wavelengths.

The influence of GLP on the LOS and LOS on the GLP affinity towards HSA, gHSA$_{GLC}$ and gHSA$_{FRC}$ was studied by comparing the quenching curves of albumins in the presence of LOS in the binary LOS-HSA, LOS-gHSA$_{GLC}$, LOS-gHSA$_{FRC}$ and ternary complexes LOS-HSA-GLP$_{const}$, LOS-gHSA$_{GLC}$-GLP$_{const}$, LOS-gHSA$_{FRC}$-GLP$_{const}$ (Figure 4), and in the presence of GLP in the binary GLP-HSA, GLP-gHSA$_{GLC}$, GLP-gHSA$_{FRC}$ and ternary complexes GLP-HSA-LOS$_{const}$, GLP-gHSA$_{GLC}$-LOS$_{const}$, GLP-gHSA$_{FRC}$-LOS$_{const}$ (Figure 5).

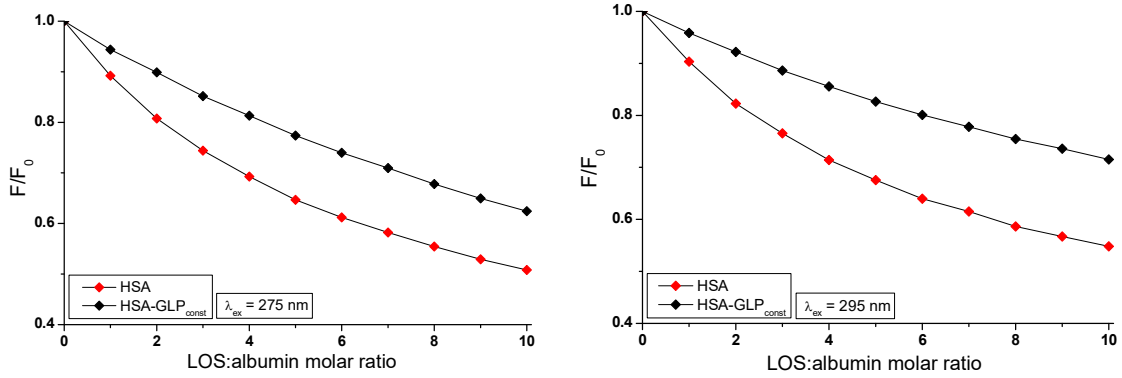

(**a**) (**b**)

Preprints.org (www.preprints.org) | NOT PEER-REVIEWED | Posted: 5 August 2024 doi:10.20944/preprints202408.0250.v1

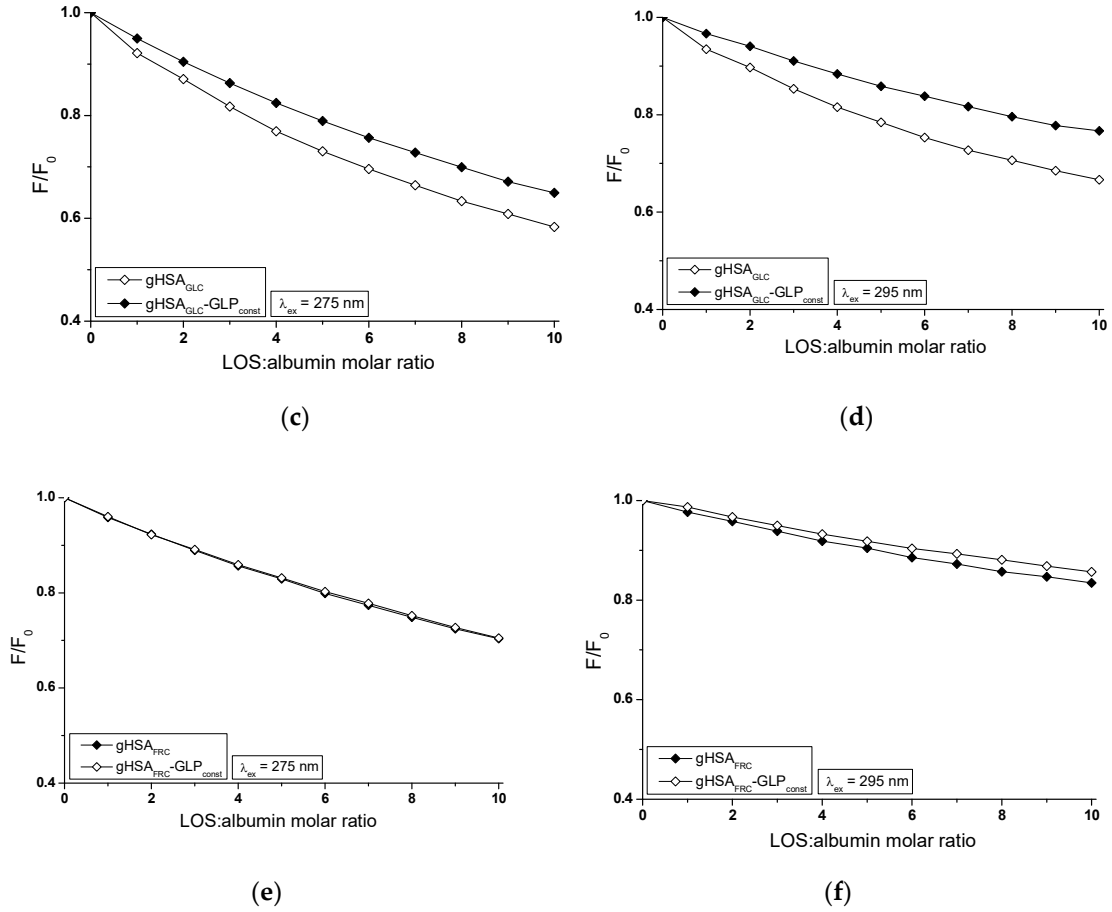

Figure 4. Quenching fluorescence of HSA (**a**, **b**), gHSA$_{GLC}$ (**c**, **d**) and gHSA$_{FRC}$ (**e**, **f**) by LOS and in the presence of GLP at 5 × 10^{-6} mol·L^{-1} concentration. LOS concentration varied from 5 × 10^{-6} mol·L^{-1} to 5 × 10^{-5} mol·L^{-1}. The proteins concentration: 5 × 10^{-6} mol·L^{-1}; λ_{ex} = 275 nm (**a**, **c**, **e**) and λ_{ex} = 295 nm (**b**, **d**, **f**); error bars, indicating the standard deviation, are smaller than the symbols used in the plots.

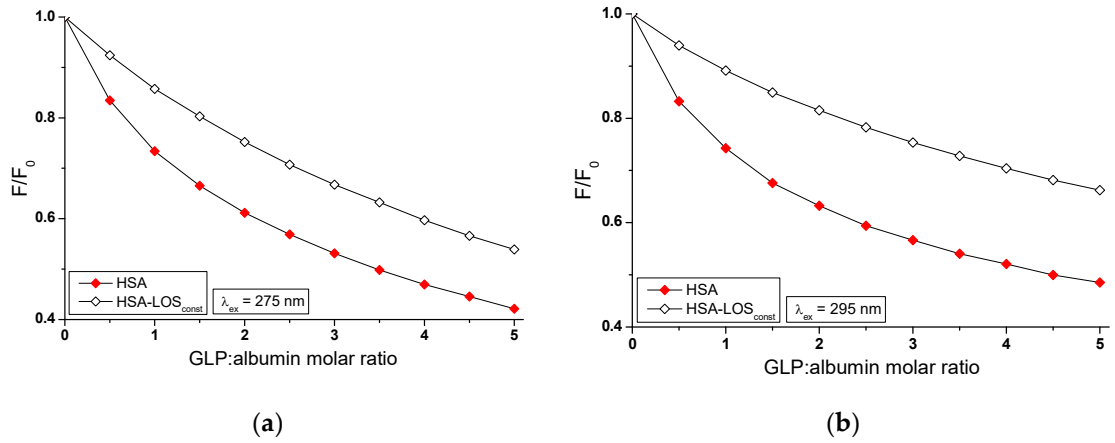

 doi:10.20944/preprints202408.0250.v1

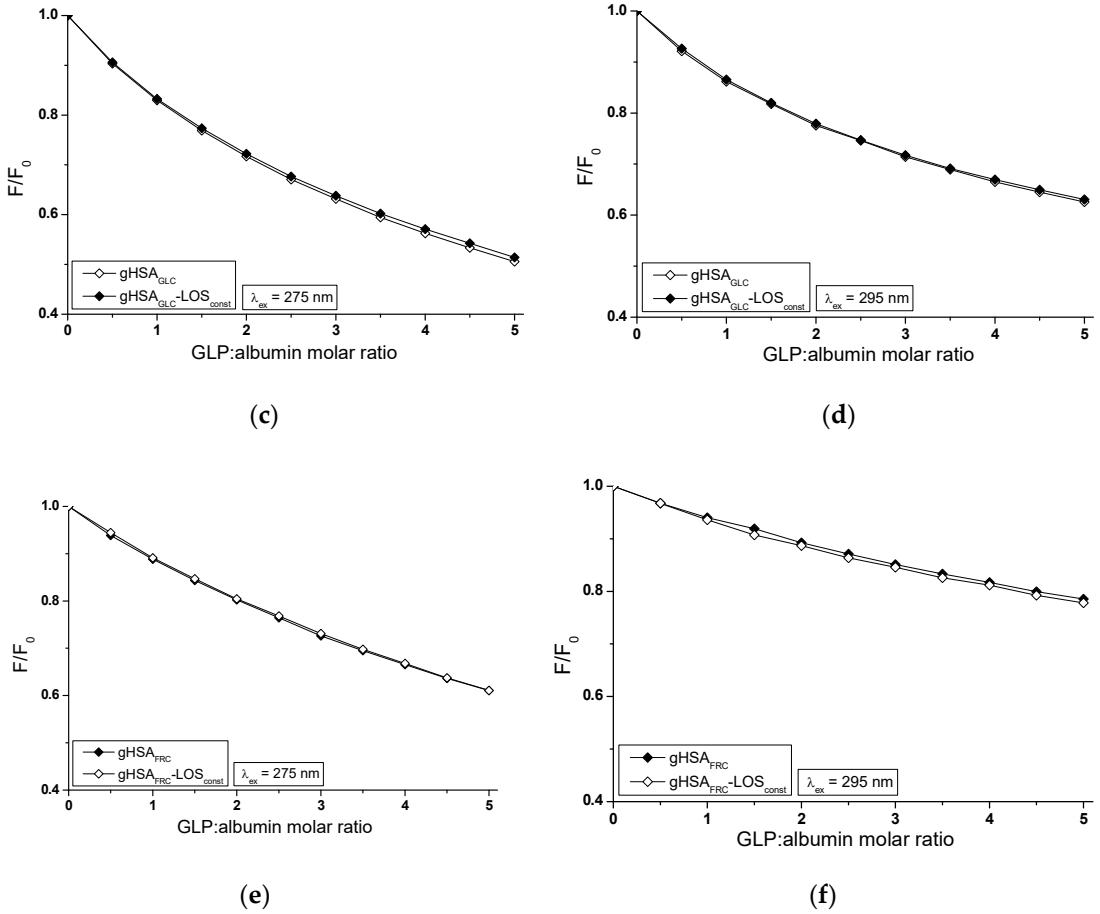

Figure 5. Quenching fluorescence of HSA (**a**, **b**), gHSA$_{GLC}$ (**c**, **d**) and gHSA$_{FRC}$ (**e**, **f**) by GLP and in the presence of LOS at 5 × 10^{-6} mol·L^{-1} concentration. GLP concentration varied from 2.5 × 10^{-6} mol·L^{-1} to 2.5 × 10^{-5} mol·L^{-1}. Protein concentration: 5 × 10^{-6} mol·L^{-1}; λ_{ex} = 275 nm (**a**, **c**, **e**) and λ_{ex} = 295 nm (**b**, **d**, **f**); error bars, indicating the standard deviation, are smaller than the symbols used in the plots.

The fluorescence quenching observed in the LOS-HSA-GLP$_{const}$ (Figures 4a,b), LOS-gHSA$_{GLC}$-GLP$_{const}$ (Figures 4c,d) and GLP-HSA-LOS$_{const}$ (Figures 5a,b) systems differs from the quenching observed in the binary systems LOS-HSA (Figures 4a,b), LOS-gHSA$_{GLC}$ (Figures 4c,d) and GLP-HSA (Figures 5a,b), respectively. The quenching of HSA and gHSA$_{GLC}$ by LOS and HSA by GLP at maximum concentration is more pronounced by 11.64% (Figure 4a), 6.64% (Figure 4c), 16.69% (Figure 4b), 10.04% (Figure 4d), 11.76% (Figure 5a), and 17.7%% (Figure 5b) compared to the systems with an additional ligand added to the binary system. An additional pharmaceutical in the system likely complicates the interaction between LOS-HSA and LOS-gHSA$_{GLC}$ (or GLP-HSA) or interferes with forming these complexes. GLP (or LOS) may cause the displacement of LOS (or GLP) from its complex with non- and glycated HSA. This effect may arise from competitive binding sites on albumin, steric hindrance, or conformational alterations of the macromolecule induced by the binding of the second ligand. Furthermore, the differing affinities and binding dynamics of GLP and LOS for albumin could result in preferential binding of one ligand over the other, thereby influencing the observed quenching effect. In contrast, the absence of differences in the quenching of intrinsic fluorescence of glycated albumin by LOS or GLP in the binary systems LOS-gHSA$_{FRC}$ (Figures 4e,f), GLP-gHSA$_{GLC}$ (Figures 5c,d), and GLP-gHSA$_{FRC}$ (Figures 5e,f) compared to the ternary systems LOS-gHSA$_{FRC}$-GLP$_{const}$ (Figures 4e,f), GLP-gHSA$_{GLC}$-LOS$_{const}$ (Figures 5c,d), and GLP-gHSA$_{FRC}$-LOS$_{const}$ (Figures 5e,f) suggests that glycation, particularly glycation of albumin by fructose, alters the macromolecule's structure and/or binding characteristics. This modification prevents the additional drug – GLP in the LOS-gHSA$_{FRC}$ complex or LOS in the GLP-gHSA$_{GLC}$ and GLP-gHSA$_{FRC}$ complexes – from competing for the binding site with LOS and GLP and prevents the displacement of drugs already bound in the gHSA$_{GLC}$ and gHSA$_{FRC}$ molecules.

 doi:10.20944/preprints202408.0250.v1

Additionally, the study on the LOS-HSA, LOS-gHSA$_{GLC}$, GLP-HSA, and LOS-HSA-GLP$_{const}$ system revealed that an increase in drug concentration leads to a hypsochromic shift ($\Delta\lambda_{max}$) of the fluorescence emission band relative to the maximum emission of unbound albumin. The hypsochromic shift indicates an increase in the hydrophobic nature of the fluorophore environment due to drug interaction with albumin. It also suggests the possibility of hydrophobic interactions between the aromatic rings of LOS and GLP molecules and the aromatic rings of amino acid residues. The more pronounced hypsochromic shift upon excitation of albumin fluorescence at λ_{ex} = 275 nm than at λ_{ex} = 295 nm indicates a less polar environment not only around Trp-214 but also around tyrosyl residues. The more substantial $\Delta\lambda_{max}$ shift towards the blue in the double systems compared to the triple systems, i.e., in the LOS-HSA system compared to LOS-HSA-GLP$_{const}$ by 5 nm, LOS-gHSA$_{GLC}$ compared to LOS-gHSA$_{GLC}$-GLP$_{const}$ by 4 nm, and GLP-HSA compared to GLP-HSA-GLP$_{const}$ by 6 nm, and for non-modified compared to glycated albumin, may indicate a decrease in the hydrophobic nature of the environment of tryptophan or/and tyrosyl residues of albumin after glycation and in the presence of an additional drug in the drug-albumin system.

The quenching mechanism of losartan and glipizide interaction with both non-glycated and glycated serum albumin was determined using the Stern-Volmer plots. The analysis encompassed the binary systems LOS-HSA, LOS-gHSA$_{GLC}$, LOS-gHSA$_{FRC}$ (Figure 6a), GLP-HSA, GLP-gHSA$_{GLC}$, GLP-gHSA$_{FRC}$ (Figure 6b), as well as the ternary systems LOS-HSA-GLP$_{const}$, LOS-gHSA$_{GLC}$-GLP$_{const}$, LOS-gHSA$_{FRC}$-GLP$_{const}$ (Figure 6c), GLP-HSA-LOS$_{const}$, GLP-gHSA$_{GLC}$-LOS$_{const}$, GLP-gHSA$_{FRC}$-LOS$_{const}$ (Figure 6d) at λ_{ex} = 275 nm (Figure 6) and λ_{ex} = 295 nm (Figure S2, Supplementary Materials).

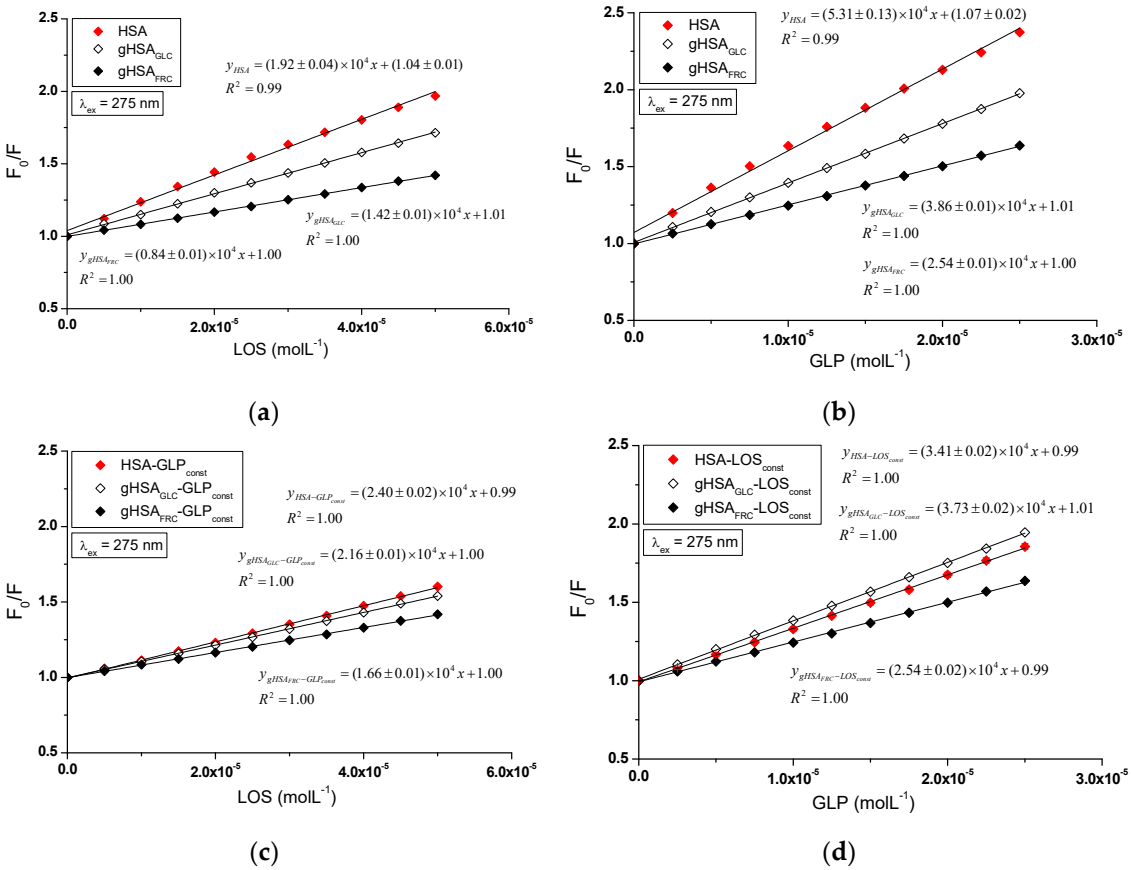

Figure 6. The Stern-Volmer curves for the binary (**a**) LOS-HSA, LOS-gHSA$_{GLC}$, LOS-gHSA$_{FRC}$; (**b**) GLP-HSA, GLP-gHSA$_{GLC}$, GLP-gHSA$_{FRC}$ and ternary systems (**c**) LOS-HSA-GLP$_{const}$, LOS-gHSA$_{GLC}$-GLP$_{const}$, LOS-gHSA$_{FRC}$-GLP$_{const}$; (**d**) GLP-HSA-LOS$_{const}$, GLP-gHSA$_{GLC}$-LOS$_{const}$, GLP-gHSA$_{FRC}$-LOS$_{const}$; λ_{ex} = 275 nm; error bars are smaller than the symbols used in the plots.

 doi:10.20944/preprints202408.0250.v1

The dependence of $\frac{F_0}{F}$ on LOS or GLP concentration in the binary and ternary systems at λ_{ex} = 275 nm (Figure 6) and λ_{ex} = 295 nm (Figure S2, Supplementary Materials) demonstrated a linear correlation for ligand-albumin complexes. The linear Stern-Volmer plots for the ligand-albumin and ligand-albumin-ligand$_{const}$ system may indicate a dynamic (collisional) or static quenching mechanism of fluorescence for both non-modified (HSA) and glycated albumins (gHSA$_{GLC}$, gHSA$_{FRC}$). According to the literature, the ligand penetrates the macromolecule's environment in dynamic quenching, and fluorescence quenching is caused by the collision between the quencher molecule and the albumin fluorophore(s). In contrast, static quenching leads to a decrease in the intensity of emitted fluorescence when the ligand binds to the fluorophore molecule in its ground (non-excited) state, thereby reducing the population of fluorophores capable of being excited [25].

Tables 1 and 2 present the Stern-Volmer constants K_{SV}, the bimolecular quenching rate constant k_q, and the fractional accessible protein fluorescence f_a calculated for binary (ligand-albumin) and ternary (ligand-albumin-ligand$_{const}$) systems at λ_{ex} = 275 nm and λ_{ex} = 295 nm.

Table 1. Stern-Volmer constants K_{SV} (L·mol^{-1}), fractional accessible albumin fluorescence f_a, and the bimolecular quenching rate constant k_q (L·mol^{-1}·s^{-1}) calculated for LOS-HSA, LOS-gHSA$_{GLC}$, LOS-gHSA$_{FRC}$ and LOS-HSA-GLP$_{const}$, LOS-gHSA$_{GLC}$-GLP$_{const}$, LOS-gHSA$_{FRC}$-GLP$_{const}$; λ_{ex} = 275 nm and λ_{ex} = 295 nm.

λ_{ex} = 275 nm	**K_{SV} ± RSD *) × 10^4 (L·mol^{-1})**	**f_a ± RSD *)**	**[a] k_q ± RSD *) × 10^{12} (L·mol^{-1}·s^{-1})**
LOS-HSA	1.92 ± 0.04	0.96 ± 0.01	3.20 ± 0.07
LOS-gHSA$_{GLC}$	1.42 ± 0.01	0.99	2.36 ± 0.02
LOS-gHSA$_{FRC}$	0.84 ± 0.01	1.00	1.40 ± 0.01
LOS-HSA-GLP$_{const}$	2.40 ± 0.02	1.01	4.00 ± 0.03
LOS-gHSA$_{GLC}$-GLP$_{const}$	2.16 ± 0.01	1.00	3.61 ± 0.01
LOS-gHSA$_{FRC}$-GLP$_{const}$	1.66 ± 0.01	1.00	2.77 ± 0.02
λ_{ex} = 295 nm	**K_{SV} ± RSD *) × 10^4 (L·mol^{-1})**	**f_a ± RSD *)**	**[a] k_q ± RSD *) × 10^{12} (L·mol^{-1}·s^{-1})**
LOS-HSA	1.64 ± 0.05	0.96 ± 0.02	2.71 ± 0.09
LOS-gHSA$_{GLC}$	0.99 ± 0.02	0.98 ± 0.01	1.66 ± 0.03
LOS-gHSA$_{FRC}$	0.40 ± 0.01	1.00	0.66 ± 0.01
LOS-HSA-GLP$_{const}$	1.59 ± 0.02	0.99	2.65 ± 0.03
LOS-gHSA$_{GLC}$-GLP$_{const}$	1.24 ± 0.02	1.00	2.07 ± 0.03
LOS-gHSA$_{FRC}$-GLP$_{const}$	0.68 ± 0.01	1.00	1.13 ± 0.02

*) Relative Standard Deviation; [a] calculated using: $k_q = \frac{K_{SV}}{\tau_0}$, where: τ_0 = 6.0 × 10^{-9} s [26]—the fluorescence lifetime of albumin in the absence of a quencher.

Table 2. Stern-Volmer constants K_{SV} (L·mol^{-1}), fractional accessible protein fluorescence f_a, and the bimolecular quenching rate constant k_q (L·mol^{-1}·s^{-1}) calculated for GLP-HSA, GLP-gHSA$_{GLC}$, GLP-gHSA$_{FRC}$ and GLP-HSA-LOS$_{const}$, GLP-gHSA$_{GLC}$-LOS$_{const}$, GLP-gHSA$_{FRC}$-LOS$_{const}$; λ_{ex} = 275 nm and λ_{ex} = 295 nm.

λ_{ex} = 275 nm	**K_{SV} ± RSD *) × 10^4 (L·mol^{-1})**	**f_a ± RSD *)**	**[a] k_q ± RSD *) × 10^{12} (L·mol^{-1}·s^{-1})**
GLP-HSA	5.31 ± 0.13	0.93 ± 0.02	8.85 ± 0.20
GLP-gHSA$_{GLC}$	3.86 ± 0.01	0.99	6.44 ± 0.02
GLP-gHSA$_{FRC}$	2.54 ± 0.01	1.00	4.23 ± 0.03
GLP-HSA-LOS$_{const}$	3.41 ± 0.02	1.01	5.69 ± 0.04
GLP-gHSA$_{GLC}$-LOS$_{const}$	3.73 ± 0.02	0.99	6.21 ± 0.03
GLP-gHSA$_{FRC}$-LOS$_{const}$	2.54 ± 0.02	1.01	4.23 ± 0.04
λ_{ex} = 295 nm	**K_{SV} ± RSD *) × 10^4 (L·mol^{-1})**	**f_a ± RSD *)**	**[a] k_q ± RSD *) × 10^{12} (L·mol^{-1}·s^{-1})**
GLP-HSA	4.05 ± 0.23	0.89 ± 0.02	6.76 ± 0.39
GLP-gHSA$_{GLC}$	2.34 ± 0.07	0.97 ± 0.01	3.91 ± 0.12
GLP-gHSA$_{FRC}$	1.09 ± 0.02	0.99	1.82 ± 0.03
GLP-HSA-LOS$_{const}$	2.02 ± 0.03	0.98 ± 0.01	3.36 ± 0.06
GLP-gHSA$_{GLC}$-LOS$_{const}$	2.31 ± 0.07	0.97 ± 0.01	3.84 ± 0.12

 doi:10.20944/preprints202408.0250.v1

GLP-gHSA$_{FRC}$-LOS$_{const}$	1.13 ± 0.02	0.99	1.88 ± 0.04

*) Relative Standard Deviation; a) calculated using: $k_q = \frac{K_{SV}}{\tau_0}$, where: $\tau_0 = 6.0 \times 10^{-9}$ s [26].

The magnitude of the determined fluorescence quenching rate constants k_q (10^{12}) for the investigated systems indicates a static fluorescence quenching mechanism in the LOS-albumin, LOS-albumin-GLP$_{const}$ (Table 1) and GLP-albumin, GLP-albumin-LOS$_{const}$ systems (Table 2). According to Lakowicz, for collisional fluorescence quenching, the maximum value of the constant k_q in an aqueous solution is 2×10^{10} (L·mol^{-1}·s^{-1}) [27].

The Stern-Volmer constant serves as a means to assess the accessibility of the quencher to the excited fluorophore. A higher K_{SV} value indicates a greater availability of ligand molecules in the macromolecule, which leads to the formation of a complex in the excited state [28]. Glycation of HSA by glucose and fructose results in a decrease in the Stern-Volmer constant in both binary (LOS-albumin, GLP-albumin) and ternary systems (LOS-albumin-GLP$_{const}$) at excitation wavelengths of 275 nm and 295 nm. This indicates a lower quenching efficiency of glycated albumin fluorophores compared to non-modified albumin by losartan (Table 1). In the ternary system (GLP-albumin-LOS$_{const}$), fructose-induced glycation decreased K_{SV}, whereas glucose-induced glycation increased K_{SV} (Table 2). The K_{SV} values determined for the system in the presence of an additional drug (LOS-albumin-GLP$_{const}$) are higher than those for the LOS-albumin system, both for unmodified and glycated albumin at λ_{ex} = 275 nm. At λ_{ex} = 295 nm, the same effect of increasing K_{SV} is observed only for the system with glycated albumin, while the presence of GLP in the LOS-HSA system caused a slight decrease in K_{SV} (Table 1). Conversely, the K_{SV} values determined for the system in the presence of an additional drug (GLP-albumin-LOS$_{const}$ complex) are lower for HSA and gHSA$_{GLC}$ at λ_{ex} = 275 nm and λ_{ex} = 295 nm. In contrast, for gHSA$_{FRC}$, they remain unchanged at λ_{ex} = 275 nm or are higher at λ_{ex} = 295 nm (Table 2). At both excitation wavelengths (λ_{ex} = 275 nm and λ_{ex} = 295 nm), GLP complexes exhibit higher K_{SV} values than to LOS complexes, indicating greater quenching efficiency. GLP molecules are closer to fluorophores of non-modified and glycated albumin than LOS molecules in binary and ternary complexes. It is also observed that K_{SV} values are generally higher at λ_{ex} = 275 nm compared to λ_{ex} = 295 nm. The bimolecular quenching rate constants (k_q) align with the trends observed in K_{SV}. Most complexes display fractional accessibility (f_a) close to or equal to 1, suggesting near-complete accessibility of the fluorophore to the quencher, with GLP-HSA showing the lowest accessibility (Table 2).

The nature of ligand binding to albumin (specificity of binding sites within the various classes of binding sites) was determined based on the binding isotherms (saturation curves) of LOS and GLP to non-glycated and glycated HSA in binary (Figures 7 ab) and ternary systems (Figures 7cd).

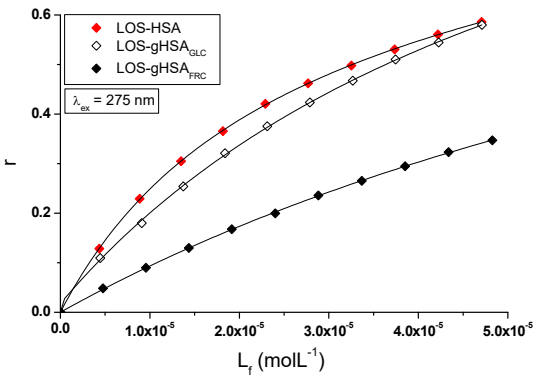

(**a**)

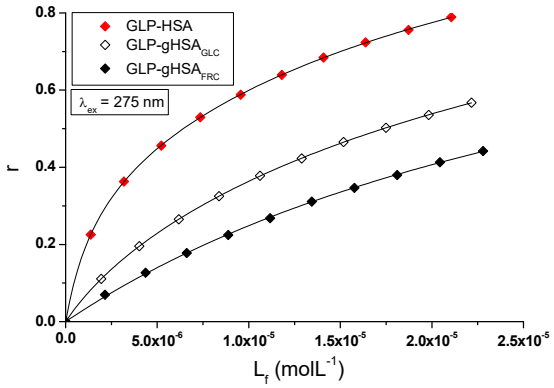

(**b**)

 doi:10.20944/preprints202408.0250.v1

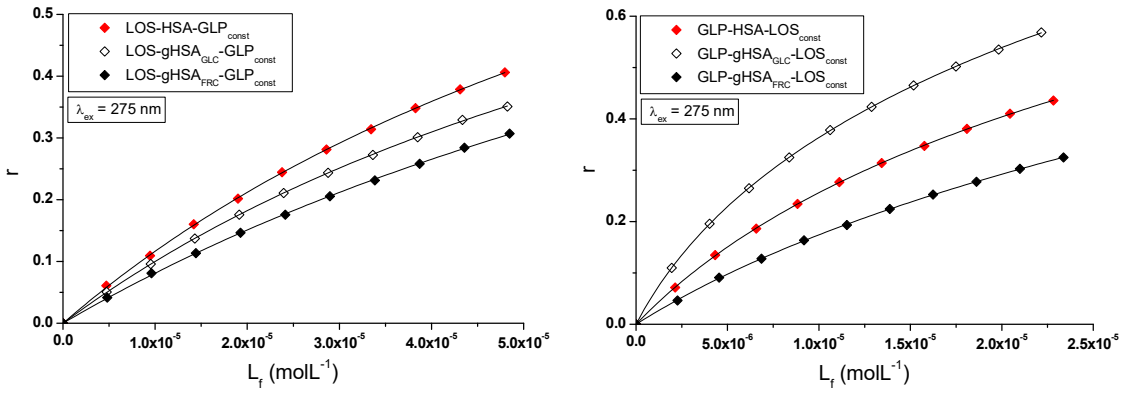

(**c**) (**d**)

Figure 7. Binding isotherms of HSA, gHSA$_{GLC}$ and gHSA$_{FRC}$ at 5 × 10^{-6} mol·L^{-1} concentration with LOS at 5 × 10^{-6} mol·L^{-1} to 5 × 10^{-5} mol·L^{-1} and GLP at 2.5 × 10^{-6} mol·L^{-1} to 2.5 × 10^{-5} mol·L^{-1} concentrations in the binary (**a**) LOS-HSA, LOS-gHSA$_{GLC}$, LOS-gHSA$_{FRC}$; (**b**) GLP-HSA, GLP-gHSA$_{GLC}$, GLP-gHSA$_{FRC}$ and ternary systems (**c**) LOS-HSA-GLP$_{const}$, LOS-gHSA$_{GLC}$-GLP$_{const}$, LOS-gHSA$_{FRC}$-GLP$_{const}$; with GLP at 5 × 10^{-6} mol·L^{-1} concentration, (**d**) GLP-HSA-LOS$_{const}$, GLP-gHSA$_{GLC}$-LOS$_{const}$, GLP-gHSA$_{FRC}$-LOS$_{const}$ with LOS at 5 × 10^{-6} mol·L^{-1} concentration, λ_{ex} = 275 nm; error bars are smaller than the symbols used in the plots.

For LOS-HSA, LOS-gHSA$_{GLC}$, LOS-gHSA$_{FRC}$ (Figure 7a), GLP-HSA, GLP-gHSA$_{GLC}$, GLP-gHSA$_{FRC}$ (Figure 7b), LOS-HSA-GLP$_{const}$, LOS-gHSA$_{GLC}$-GLP$_{const}$, LOS-gHSA$_{FRC}$-GLP$_{const}$ (Figure 7c) and GLP-HSA-LOS$_{const}$, GLP-gHSA$_{GLC}$-LOS$_{const}$, GLP-gHSA$_{FRC}$-LOS$_{const}$ (Figure 7d) complexes at λ_{ex} = 275 nm (Figure 7) and at λ_{ex} = 295 nm (Figure S3, Supplementary Materials), the course of the saturation curves is not linear across the entire range of ligand concentrations, as each of the binding isotherms exhibits an exponentially increasing course and does not reach a "plateau". Therefore, based on the analyzed plots, it can be inferred that LOS and GLP nonspecifically interact with the hydrophobic fragments of the surface of non-glycated and glycated albumin in both binary and ternary systems and specifically saturate the binding sites within the protein molecule, as confirmed by the literature [29]. Specific binding is characterized by high affinity and low binding capacity, whereas nonspecific binding is characterized by low affinity and unlimited ligand binding capacity of the ligand [29]. The physicochemical compatibility of both molecules determines the binding of ligands to serum albumin. Small structural changes in the protein molecule can influence the mutual interaction of the drug with albumin, which in turn affects the binding parameters.

Specific binding of losartan and glipizide to non-modified and glycated albumin in the complexes LOS-HSA, LOS-gHSA$_{GLC}$, LOS-gHSA$_{FRC}$, GLP-HSA, GLP-gHSA$_{GLC}$, GLP-gHSA$_{FRC}$, LOS-HSA-GLP$_{const}$, LOS-gHSA$_{GLC}$-GLP$_{const}$, LOS-gHSA$_{FRC}$-GLP$_{const}$ and GLP-HSA-LOS$_{const}$, GLP-gHSA$_{GLC}$-LOS$_{const}$, GLP-gHSA$_{FRC}$-LOS$_{const}$ were quantitatively analyzed by calculating the association constant K_a using the Scatchard equation (with ligand-bound fraction concentration as the independent variable) (Figure 8), the Klotz equation (with the inverse of the free ligand fraction concentration as the independent variable) (Figure 9), and through non-linear regression based on the Levenberg-Marquardt algorithm, i.e., binding isotherms (Figure 7). Additionally, Hill's coefficients (n_H), representing cooperativity, were determined using the linear Hill plot (with the logarithm of the free ligand fraction concentration as the independent variable) (Figure 10). Changes in the high-affinity binding of LOS and GLP to non-glycated and glycated albumin in binary and ternary systems, based on K_a, the number of LOS and GLP molecules bound to one mole of the macromolecule at a specific binding site (n), as well as Hill's coefficient of cooperativity, are summarized in Tables 3 and 4, respectively (λ_{ex} = 275 nm, λ_{ex} = 295 nm).

Table 3. Association constants K_a (L·mol^{-1}), mean number of LOS molecule bound with one molecule of HSA, gHSA$_{GLC}$ and gHSA$_{FRC}$ (n), the Hill's coefficient (n_H) in the binary (LOS-HSA, LOS-

 doi:10.20944/preprints202408.0250.v1

gHSA$_{GLC}$, LOS-gHSA$_{FRC}$) and ternary system (LOS-HSA-GLP$_{const}$, LOS-gHSA$_{GLC}$-GLP$_{const}$, LOS-gHSA$_{FRC}$-GLP$_{const}$); λ_{ex} = 275 nm and λ_{ex} = 295 nm.

	Scatchard Method		Klotz Method		Hill Method
λ_{ex} = 275 nm	**K_a ± RSD *) × 10^4 (L·mol^{-1})**	**n ± RSD *)**	**K_a ± RSD *) × 10^4 (L·mol^{-1})**	**n ± RSD *)**	**n_H ± RSD *)**
LOS-HSA	3.76 ± 0.05	0.91 ± 0.02	3.78 ± 0.02	0.91 ± 0.01	0.94
LOS-gHSA$_{GLC}$	2.31 ± 0.19	1.09 ± 0.12	2.90 ± 0.16	0.93 ± 0.08	1.04 ± 0.02
LOS-gHSA$_{FRC}$	0.93 ± 0.05	1.12 ± 0.07	1.10 ± 0.07	0.97 ± 0.07	1.02 ± 0.01
LOS-HSA-GLP$_{const}$	1.20 ± 0.06	1.11 ± 0.07	1.39 ± 0.09	0.98 ± 0.08	1.02 ± 0.01
LOS-gHSA$_{GLC}$-GLP$_{const}$	1.10 ± 0.01	1.02 ± 0.01	1.13 ± 0.01	0.99 ± 0.01	1.00
LOS-gHSA$_{FRC}$-GLP$_{const}$	0.89 ± 0.04	1.01 ± 0.05	0.93 ± 0.03	0.97 ± 0.04	1.00 ± 0.01
λ_{ex} = 295 nm	**K_a ± RSD *) × 10^4 (L·mol^{-1})**	**n ± RSD *)**	**K_a ± RSD *) × 10^4 (L·mol^{-1})**	**n ± RSD *)**	**n_H ± RSD *)**
LOS-HSA	3.61 ± 0.07	0.92 ± 0.03	3.49 ± 0.04	0.94 ± 0.02	0.95 ± 0.01
LOS-gHSA$_{GLC}$	2.40 ± 0.26	1.12 ± 0.17	3.20 ± 0.23	0.93 ± 0.10	1.06 ± 0.03
LOS-gHSA$_{FRC}$	0.89 ± 0.07	1.13 ± 0.11	1.06 ± 0.10	0.97 ± 0.10	1.02 ± 0.01
LOS-HSA-GLP$_{const}$	1.16 ± 0.02	0.97 ± 0.03	1.16 ± 0.03	0.97 ± 0.03	0.99
LOS-gHSA$_{GLC}$-GLP$_{const}$	0.91 ± 0.08	1.12 ± 0.12	1.09 ± 0.12	0.96 ± 0.12	1.02 ± 0.01
LOS-gHSA$_{FRC}$-GLP$_{const}$	a) 0.59 ± 0.01	a) 0.85 ± 0.01	- **)	- **)	1.20 ± 0.02

*) Relative Standard Deviation; a) determined by non-linear regression using binding isotherms; **) impossible to determine .

Table 4. Association constants K_a (L·mol^{-1}), mean number of GLP molecule bound with one molecule of HSA, gHSA$_{GLC}$ and gHSA$_{FRC}$ (n), the Hill's coefficient (n_H) in the binary (GLP-HSA, GLP-gHSA$_{GLC}$, GLP-gHSA$_{FRC}$) and ternary system (GLP-HSA-LOS$_{const}$, GLP-gHSA$_{GLC}$-LOS$_{const}$, GLP-gHSA$_{FRC}$-LOS$_{const}$); λ_{ex} = 275 nm and λ_{ex} = 295 nm.

	Scatchard Method		Klotz Method		Hill Method
λ_{ex} = 275 nm	**K_a ± RSD *) × 10^4 (L·mol^{-1})**	**n ± RSD *)**	**K_a ± RSD *) × 10^4 (L·mol^{-1})**	**n ± RSD *)**	**n_H ± RSD *)**
GLP-HSA	a) 57.84 ± 3.01 a) 3.44 ± 0.31	a) 0.41 ± 0.02 a) 0.97 ± 0.02	25.38 ± 0.04	0.85 ± 0.03	0.92 ± 0.03
GLP-gHSA$_{GLC}$	6.66 ± 0.30	0.93 ± 0.06	7.48 ± 0.17	0.86 ± 0.03	0.96 ± 0.01
GLP-gHSA$_{FRC}$	3.27 ± 0.17	1.02 ± 0.07	3.82 ± 0.17	0.91 ± 0.05	1.00 ± 0.01
GLP-HSA-LOS$_{const}$	3.96 ± 0.08	0.91 ± 0.02	4.07 ± 0.06	0.89 ± 0.02	0.97
GLP-gHSA$_{GLC}$-LOS$_{const}$	6.58 ± 0.27	0.94 ± 0.06	7.26 ± 0.12	0.88 ± 0.02	0.97 ± 0.01
GLP-gHSA$_{FRC}$-LOS$_{const}$	2.45 ± 0.07	0.89 ± 0.03	2.35 ± 0.09	0.92 ± 0.04	0.98 ± 0.01
λ_{ex} = 295 nm	**K_a ± RSD *) × 10^4 (L·mol^{-1})**	**n ± RSD *)**	**K_a ± RSD *) × 10^4 (L·mol^{-1})**	**n ± RSD *)**	**n_H ± RSD *)**
GLP-HSA	a) 112.04 ± 25.01 a) 7.52 ± 1.29	a) 0.34 ± 0.05 a) 0.77 ± 0.02	36.45 ± 0.20	0.83 ± 0.03	0.84 ± 0.03
GLP-gHSA$_{GLC}$	8.40 ± 0.41	0.93 ± 0.07	9.43 ± 0.11	0.87 ± 0.02	0.96 ± 0.01
GLP-gHSA$_{FRC}$	2.69 ± 0.19	1.06 ± 0.10	3.23 ± 0.19	0.92 ± 0.07	1.01 ± 0.01
GLP-HSA-LOS$_{const}$	5.15 ± 0.22	0.97 ± 0.06	5.77 ± 0.15	0.89 ± 0.03	0.99 ± 0.01
GLP-gHSA$_{GLC}$-LOS$_{const}$	7.30 ± 0.16	0.89 ± 0.03	7.50 ± 0.09	0.88 ± 0.02	0.94
GLP-gHSA$_{FRC}$-LOS$_{const}$	2.92 ± 0.14	0.87 ± 0.05	2.69 ± 0.13	0.93 ± 0.05	0.97 ± 0.01

*) Relative Standard Deviation; a) determined by non-linear regression using binding isotherms.

The Scatchard model of ligand-protein interactions postulates that the protein molecule possesses a finite number of specific binding sites for ligands. In this case, the Scatchard dependence $\frac{r}{[L_f]} = f(r)$ is linear and intersects the x-axis of the coordinate system (the r-axis). The linear Scatchard plots for the complexes LOS-HSA, LOS-gHSA$_{GLC}$, LOS-gHSA$_{FRC}$ (Figure 8a), GLP-gHSA$_{GLC}$, GLP-gHSA$_{FRC}$ (Figure 8b), LOS-HSA-GLP$_{const}$, LOS-gHSA$_{GLC}$-GLP$_{const}$, LOS-gHSA$_{FRC}$-GLP$_{const}$ (Figure 8c)

 doi:10.20944/preprints202408.0250.v1

and GLP-HSA-LOS$_{const}$, GLP-gHSA$_{GLC}$-LOS$_{const}$, GLP-gHSA$_{FRC}$-LOS$_{const}$ (Figure 8d) at λ_{ex} = 275 nm (Figure 8) and λ_{ex} = 295 nm (Figure S4, Supplementary Materials) indicate the existence of one class of equivalent, independent binding sites for LOS and GLP in both non-modified and glycated albumin structures (or a single binding site), characterized by the same association constant K_a. A non-linear Scatchard dependence resembling a hyperbola was observed for the GLP-HSA complex excited at λ_{ex} = 275 nm (Figure 8b) and λ_{ex} = 295 nm (Figure S4b, Supplementary Materials). This phenomenon may result from the presence of more than one class of ligand-binding sites within the albumin structure (heterogeneous binding), the non-specific nature of GLP binding to HSA, and/or negative cooperativity, where the binding of the drug at one site reduces its affinity for the remaining binding sites on the macromolecule. In contrast, for the LOS-gHSA$_{FRC}$-GLP$_{const}$ complex excited at λ_{ex} = 295 nm (Figure S4c, Supplementary Materials), a "cone-shaped" Scatchard plot was obtained, which may indicate positive cooperativity or instability of losartan. Assuming the existence of two classes of binding sites, the binding parameters for GLP-HSA and LOS-gHSA$_{FRC}$-GLP$_{const}$ were determined by non-linear regression using the Levenberg-Marquardt algorithm (Tables 3 and 4).

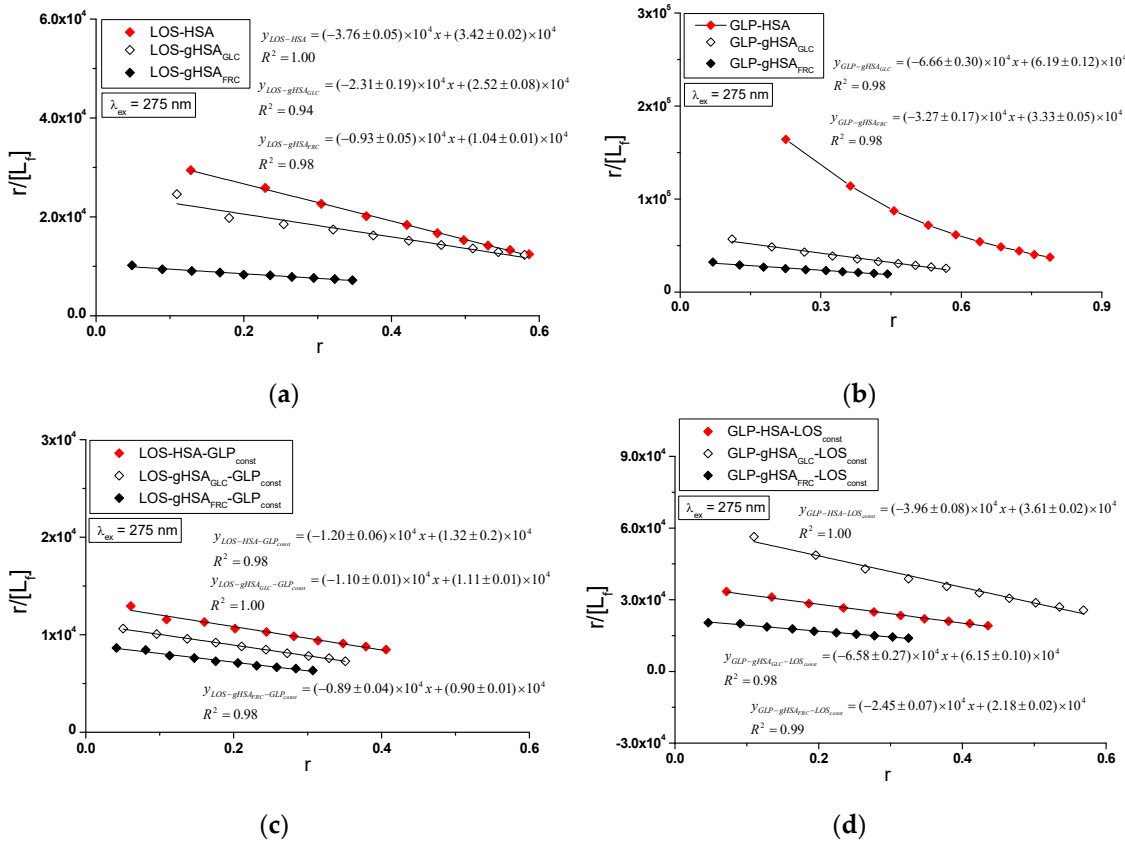

Figure 8. Scatchard plots for the binary (**a**) LOS-HSA, LOS-gHSA$_{GLC}$, LOS-gHSA$_{FRC}$; (**b**) GLP-HSA, GLP-gHSA$_{GLC}$, GLP-gHSA$_{FRC}$ and ternary systems (**c**) LOS-HSA-GLP$_{const}$, LOS-gHSA$_{GLC}$-GLP$_{const}$, LOS-gHSA$_{FRC}$-GLP$_{const}$; (**d**) GLP-HSA-LOS$_{const}$, GLP-gHSA$_{GLC}$-LOS$_{const}$, GLP-gHSA$_{FRC}$-LOS$_{const}$; λ_{ex} = 275 nm; error bars are smaller than the symbols used in the plots.

Figure 9 illustrates the linear course of the Klotz dependence $\frac{1}{r} = f(\frac{1}{[L_f]})$ for the binary (Figures 9a and b) and ternary systems (Figures 9c and d) at λ_{ex} = 275 nm, indicating the binding of ligands to albumins within a single class of binding sites. Notably, for the system LOS-gHSA$_{FRC}$-GLP$_{const}$ at λ_{ex} = 295 nm, a non-linear course of the Klotz dependence was observed (Figure S5, Supplementary Materials).

Preprints.org (www.preprints.org) | NOT PEER-REVIEWED | Posted: 5 August 2024 doi:10.20944/preprints202408.0250.v1

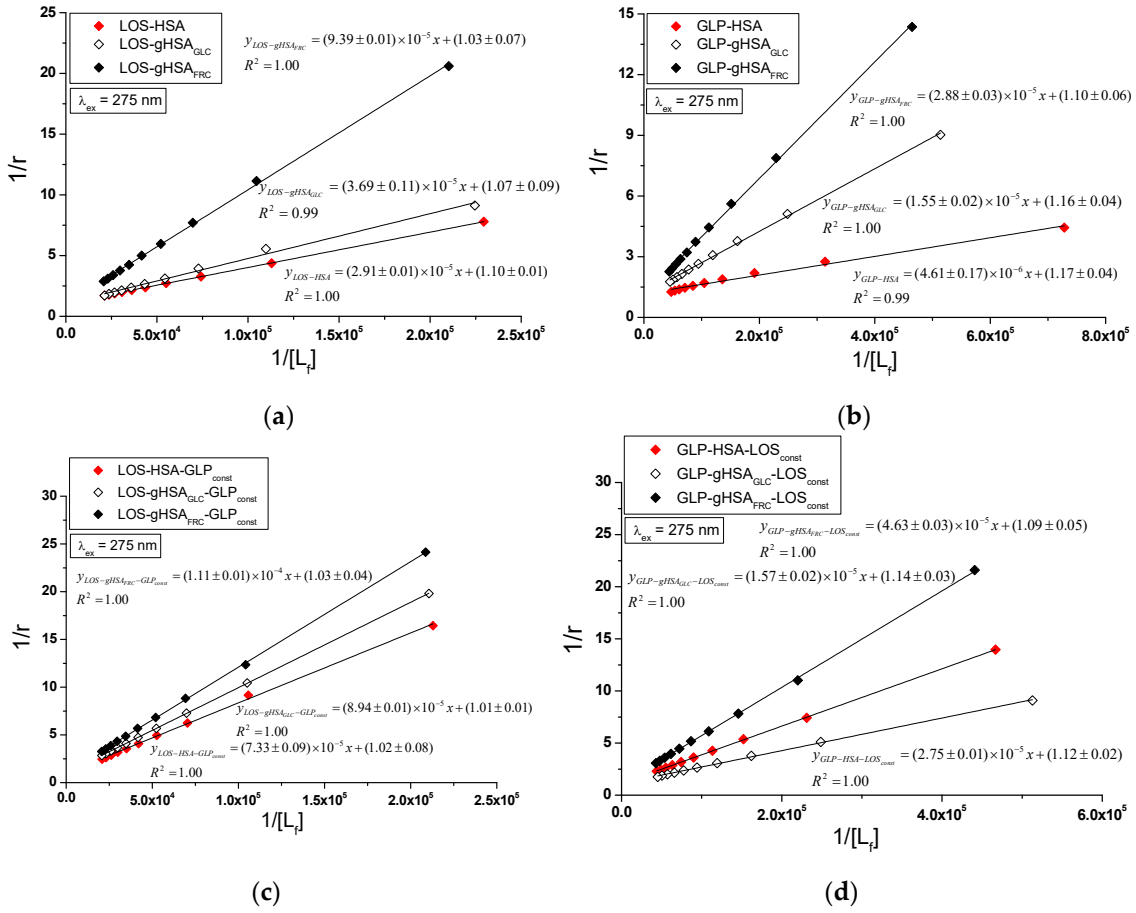

Figure 9. Klotz curves for the binary (**a**) LOS-HSA, LOS-gHSA$_{GLC}$, LOS-gHSA$_{FRC}$; (**b**) GLP-HSA, GLP-gHSA$_{GLC}$, GLP-gHSA$_{FRC}$ and ternary systems (**c**) LOS-HSA-GLP$_{const}$, LOS-gHSA$_{GLC}$-GLP$_{const}$, LOS-gHSA$_{FRC}$-GLP$_{const}$; (**d**) GLP-HSA-LOS$_{const}$, GLP-gHSA$_{GLC}$-LOS$_{const}$, GLP-gHSA$_{FRC}$-LOS$_{const}$; λ_{ex} = 275 nm; error bars are smaller than the symbols used in the plots.

In the first class of binding sites, the association constants K_a determined from the linear Scatchard and Klotz dependencies for the LOS-gHSA$_{GLC}$ and LOS-gHSA$_{FRC}$ complexes when excited at λ_{ex} = 275 nm and λ_{ex} = 295 nm are lower than those for the LOS-HSA complex (Table 3). A comparable trend was noted in the ternary system, where the K_a are lower for the complexes with glycated (LOS-gHSA$_{GLC}$-GLP$_{const}$, LOS-gHSA$_{FRC}$-GLP$_{const}$) compared to non-modified albumin (LOS-HSA-GLP$_{const}$). This suggests that albumin glycation reduces the stability of the formed complex for both the excited Trp-214 and the Tyr residues. Losartan has the lowest affinity for fructose-glycated protein (gHSA$_{FRC}$). Moreover, the presence of an additional drug, i.e., GLP, in the LOS-albumin system weakens the binding of LOS to the macromolecules, as evidenced by a decrease in K_a (Table 3). For the LOS-gHSA$_{FRC}$-GLP$_{const}$ complex excited at λ_{ex} = 295 nm, the non-linear course of the Klotz plot made it impossible to determine the binding parameters (Figure S5).

The K_a constants, determined by linear regression from the dependencies on the Klotz and the Scatchard equations, as well as based on binding isotherms, are significantly higher for the GLP-HSA compared to the GLP-gHSA$_{GLC}$ and GLP-gHSA$_{FRC}$ complex (Table 4). This suggests that glipizide has a greater affinity for non-modified than glycated albumin, forming a more stable complex. These findings align with previous studies by Koyama et al. [30], which used fluorescence quenching techniques to demonstrate that the binding capacity of hypoglycemic drugs to glycated albumin (G-HSA) was significantly lower than to non-modified HSA. Moreover, Wiglusz et al. [31] demonstrated that gliclazide, a popular hypoglycemic drug, binds more weakly to glycated albumin than its native form. These results confirm that glycation alters the protein structure and drug-binding capacity. Furthermore, Chume et al. [32] confirmed that glycation of albumin decreases its binding capacity

 doi:10.20944/preprints202408.0250.v1

for hypoglycemic drugs, which has profound implications for the pharmacokinetics and pharmacodynamics of these drugs in diabetic patients. Conversely, for the ternary system, a higher K_a was determined for GLP-gHSA$_{GLC}$-LOS$_{const}$ compared to GLP-HSA-LOS$_{const}$ and GLP-gHSA$_{FRC}$-LOS$_{const}$, indicating that glucose glycation increases the stability of the formed GLP-albumin-LOS$_{const}$ complex. Furthermore, the presence of LOS in the GLP-albumin complex generally weakens the binding of GLP to HSA and gHSA$_{FRC}$, as reflected in a decrease in K_a (Table 4). However, the presence of LOS does not significantly affect the K_a value in the complex with albumin glycated by glucose at λ_{ex} = 275 nm (K_a(GLP-gHSA$_{GLC}$) ≈ K_a(GLP-gHSA$_{GLC}$-LOS$_{const}$)).

In addition, glipizide at a 5:1 GLP:albumin molar ratio has a higher affinity for non-glycated and glycated protein than losartan at a 10:1 LOS:albumin molar ratio. This effect indicates that the transfer of energy from albumin fluorophores (Trp-214 and Tyr residues) to GLP is more efficient than to LOS in both binary (ligand-albumin) and ternary (in the presence of an additional drug at a 1:1 molar ratio, ligand-albumin-ligand$_{const}$) complexes. The number of binding sites n close to one indicates the existence of a single specific binding site for LOS and GLP in non-modified and glycated molecules (Tables 3 and 4).

To determine whether the binding of LOS and GLP to albumins affects the affinity of the ligand for other binding sites within the macromolecule, Hill's coefficient (n_H) for cooperativity was calculated based on the linear Hill plot. Figure 10 shows the linear Hill dependence $log\left(\frac{r}{1-r}\right) = f\left(log\,[L_f]\right)$ in the binary LOS-HSA, LOS-gHSA$_{GLC}$, LOS-gHSA$_{FRC}$ (Figure 10a), GLP-HSA, GLP-gHSA$_{GLC}$, GLP-gHSA$_{FRC}$ (Figure 10b), as well as the ternary systems LOS-HSA-GLP$_{const}$, LOS-gHSA$_{GLC}$-GLP$_{const}$, LOS-gHSA$_{FRC}$-GLP$_{const}$ (Figure 10c) and GLP-HSA-LOS$_{const}$, GLP-gHSA$_{GLC}$-LOS$_{const}$, GLP-gHSA$_{FRC}$-LOS$_{const}$ (Figure 10d) at λ_{ex} = 275 nm.

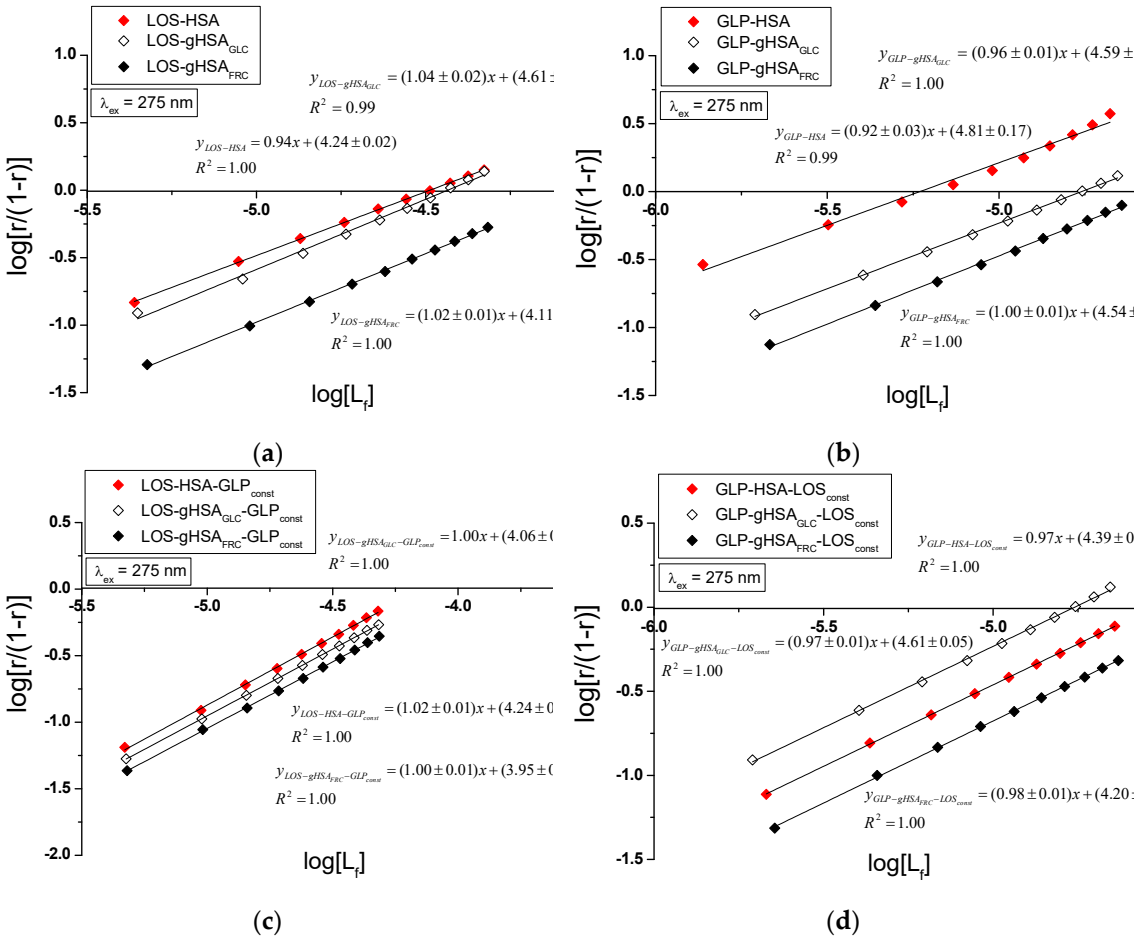

Figure 10. Hill plots for the binary (**a**) LOS-HSA, LOS-gHSA$_{GLC}$, LOS-gHSA$_{FRC}$; (**b**) GLP-HSA, GLP-gHSA$_{GLC}$, GLP-gHSA$_{FRC}$ and ternary systems (**c**) LOS-HSA-GLP$_{const}$, LOS-gHSA$_{GLC}$-GLP$_{const}$, LOS-

 doi:10.20944/preprints202408.0250.v1

gHSA$_{FRC}$-GLP$_{const}$; (**d**) GLP-HSA-LOS$_{const}$, GLP-gHSA$_{GLC}$-LOS$_{const}$, GLP-gHSA$_{FRC}$-LOS$_{const}$; λ_{ex} = 275 nm; error bars are smaller than the symbols used in the plots.

For the LOS-HSA (Table 3) and the GLP-HSA complex (Table 4), the Hill coefficient values were found to be less than one ($n_H < 1$) at both excitation wavelengths, indicating negative cooperativity. This implies that binding one LOS or GLP molecule at a binding site decreases the affinity for subsequent ligand binding at other sites on non-glycated albumin [33]. Conversely, for the LOS-gHSA$_{FRC}$-GLP$_{const}$ complex (Table 3), the Hill coefficient greater than one was observed ($n_H > 1$), suggesting positive cooperativity. Here, the binding of one LOS molecule facilitates the binding affinity for additional molecules within the LOS-gHSA$_{FRC}$-GLP$_{const}$ complex when excited at 295 nm. For the remaining systems, the Hill coefficient was approximately one ($n_H \approx 1$), indicating non-cooperative binding of LOS and GLP to the macromolecules, where the binding of one ligand molecule does not affect the binding affinity of subsequent molecules.

2.3. Investigating Ligand Interactions: Spectrophotometric Analysis of Losartan and Glipizide

There are numerous possibilities for mutual interactions between different pharmaceuticals. Some of these interactions are well-documented and thus can be easily avoided during treatment. However, other medicine interactions are often uncovered only after investigating the underlying causes of treatment failure. Understanding these interactions is crucial, as it can significantly optimize therapeutic outcomes, potentially leading to better patient care and minimizing adverse effects. In this study, in addition to spectrofluorimetry, spectrophotometric measurements were conducted to verify the hypothesis that GLP and LOS can interact not only with non-glycated (HSA) and glycated albumin (gHSA$_{GLC}$, gHSA$_{FRC}$) (as discussed in Chapter 2.2.) but also with each other.

Figure 11 shows the absorption spectra of GLP, LOS, and the drug complex (GLP+LOS), from which the absorbance values at selected wavelengths were read. The results are presented in Table 5.

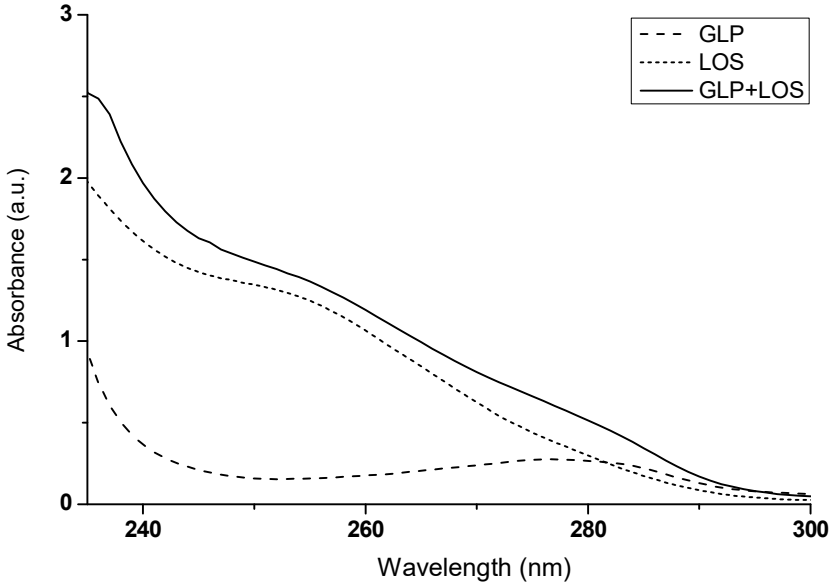

Figure 11. The absorption spectra of GLP, LOS and the drugs mixture (GLP+LOS); drug concentration is 2.5 × 10^{-5} mol·L^{-1}; the GLP to LOS molar ratio is 1:1; t = 37°C.

Table 5. The values of maximum absorbance of GLP, LOS and drugs mixture at the selected wavelengths λ = 235 nm, λ = 253 nm, and λ = 282 nm.

λ (nm)	Absorbance (a.u.)			Mathematic sum of GLP and LOS absorbance
	GLP	LOS	GLP+LOS	
235	0.9319	1.9768	2.5215	2.9087
253	0.1545	1.2960	1.4173	1.4505

 doi:10.20944/preprints202408.0250.v1

282	0.2549	0.2456	0.4509	0.5005

If the absorbance of a mixture of two substances deviates from the mathematical sum of their individual absorbances, it may indicate potential mutual interactions, as suggested by Ren et al. [34]. By observing differences in the absorbance values of GLP and LOS in their combined mixture (GLP+LOS), compared to the expected mathematical sum of their absorbances (Figure 11, Table 5), it can be inferred that GLP and LOS interact with each other. These interactions emphasize the importance of closely monitoring patients' co-administered LOS and GLP, mainly focusing on blood glucose levels, blood pressure, and renal function to ensure safe and effective therapy.

2.4. Spectropolarimetric Analysis of Glycation and Losartan Influence on Macromolecule Secondary Structure

Circular dichroism (CD) spectroscopy was used to evaluate the impact of the glycation process and the presence of losartan (LOS) on the secondary structure of human serum albumin (Figure 12). CD spectroscopy is a valuable analytical technique for assessing the secondary structure of chiral molecules, particularly proteins. It can monitor conformational protein changes, such as folding/unfolding, ligand binding, and protein-protein interactions [35]. CD measurements in the far-UV region can provide quantitative assessments of secondary structure, which can be compared to findings from X-ray crystallography or NMR studies [36].

Tables 6 and 7 present the value of non-glycated and glycated albumin mean residue ellipticity $[\theta]_{mrw}$ and the percentage content (%) of albumin secondary structure elements in the sample without (HSA, gHSA$_{GLC}$, gHSA$_{FRC}$) and in the presence of losartan at molar ratio of LOS:albumin 10:1 (LOS-HSA, LOS-gHSA$_{GLC}$, LOS-gHSA$_{FRC}$).

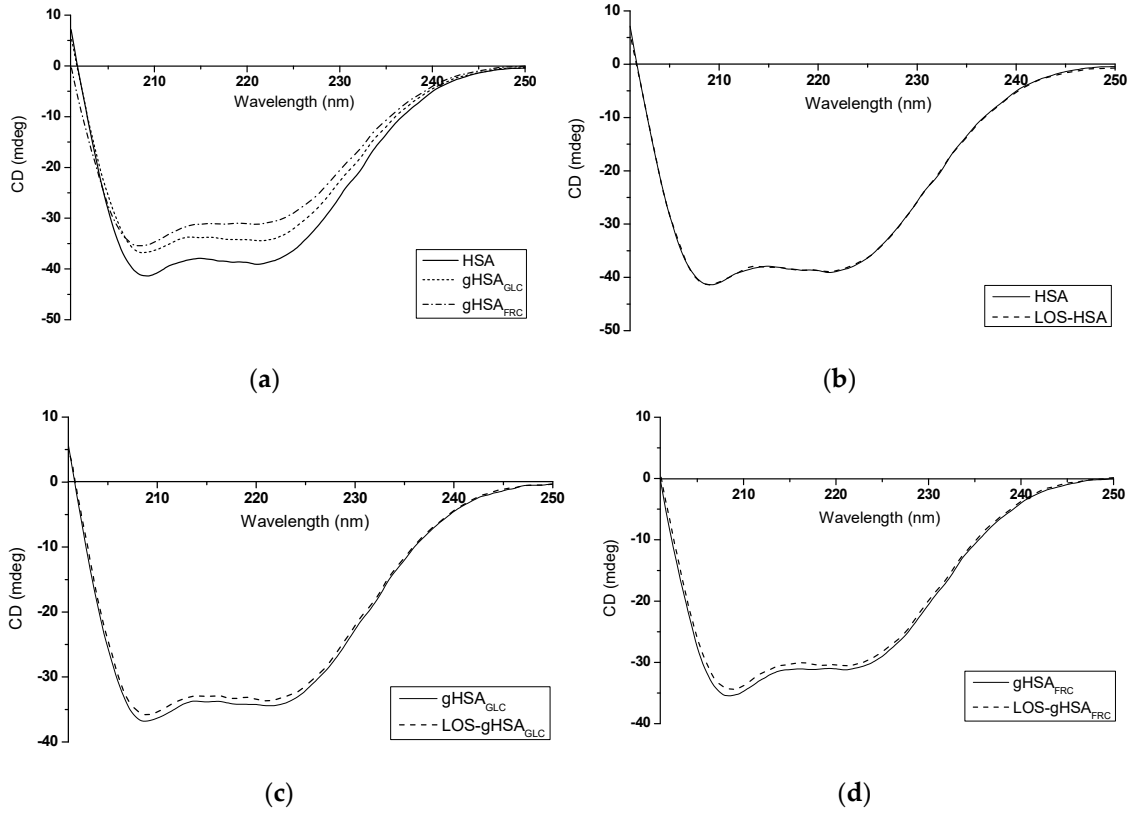

Figure 12. Far-UV CD spectra of (**a**) non-glycated (HSA) and glycated (gHSA$_{GLC}$, gHSA$_{FRC}$) human serum albumin; (**b**) HSA and LOS-HSA; (**c**) gHSA$_{GLC}$ and LOS-gHSA$_{GLC}$; (**d**) gHSA$_{FRC}$ and LOS-gHSA$_{FRC}$; protein concentration equals 5×10^{-6} mol·L^{-1}; the LOS to albumin molar ratio is 10:1; t = 37°C.

 doi:10.20944/preprints202408.0250.v1

Table 6. The values of non-glycated and glycated albumin mean residue ellipticity $[\theta]_{mrw}$ in the sample without (HSA, gHSA$_{GLC}$, gHSA$_{FRC}$) and in the presence of losartan (LOS-HSA, LOS- gHSA$_{GLC}$, LOS-gHSA$_{FRC}$).

Sample*	λ_{min} (nm)	$[\theta]_{mrw}$ (deg·cm^2·dmol^{-1})	HT (V)
HSA	209.2	−13,855.23	281.61
	221.2	−13,087.41	242.06
gHSA$_{GLC}$	208.8	−12,324.99	284.85
	221.2	−11,529.40	242.88
gHSA$_{FRC}$	208.6	−11,871.22	286.79
	221.2	−10,453.40	243.58
LOS-HSA	209.2	−13,869.50	301.08
	221.2	−13,035.94	254.15
LOS-gHSA$_{GLC}$	208.8	−11,993.66	298.99
	221.2	−11,273.80	251.65
LOS-gHSA$_{FRC}$	208.6	−11,513.06	300.09
	221.2	−10,230.25	253.13

*for the remaining complexes (GLP-HSA, GLP-gHSA$_{GLC}$, GLP-gHSA$_{FRC}$, GLP-HSA-LOS$_{const}$, GLP-gHSA$_{GLC}$-LOS$_{const}$, GLP-gHSA$_{FRC}$-LOS$_{const}$, LOS-HSA-GLP$_{const}$, LOS-gHSA$_{GLC}$-GLP$_{const}$, LOS-gHSA$_{FRC}$-GLP$_{const}$), obtaining CD spectra was impossible due to excessively weak signals likely caused by too low a concentration of GLP. This resulted in the sample absorbance exceeding the detector's capacity, leading to off-scale signals – HT (High Tension) readings outside the acceptable range.

Table 7. The percentage content (%) of non-glycated and glycated albumin secondary structure elements in the sample without (HSA, gHSA$_{GLC}$, gHSA$_{FRC}$) and in the presence of losartan (LOS-HSA, LOS-gHSA$_{GLC}$, LOS-gHSA$_{FRC}$) based on the Yang's Reference model.

	% α-Helix	% β-Sheet	% Turn	% Random
HSA	36.6	10.2	22.6	30.6
gHSA$_{GLC}$	35.7	11.1	22.4	30.8
gHSA$_{FRC}$	20.0	16.7	21.6	32.7
LOS-HSA	35.7	8.8	23.9	31.7
LOS-gHSA$_{GLC}$	35.8	9.7	23.4	31.1
LOS-gHSA$_{FRC}$	29.9	15.9	21.9	32.4

According to the data presented in Tables 6 and 7, it can be inferred that both non-glycated and glycated albumin primarily display an α-helical structure. The CD spectrum of HSA is characterized by a strong double minimum at λ_{min} = 209.2 nm and λ_{min} = 221.2 nm, which shifts slightly towards shorter wavelengths due to albumin glycation (Figure 12a, Table 6). Absorption in the region below λ = 240 nm is primarily attributed to the peptide bond, featuring a weak but broad n → π* transition centred around λ = 220 nm and a more intense π → π* transition near λ = 190 nm [36]. The reduction in mean residue ellipticity $[\theta]_{mrw}$ and CD band intensity observed, especially in glycated gHSA$_{FRC}$ compared to non-glycated HSA (Figure 12a, Table 6), may indicate a decrease in α-helix content (gHSA$_{FRC}$ 16.6%) and an increase in β-sheet content of albumin after glycation by fructose (gHSA$_{FRC}$ 6.5%) (Table 7). Mou et al. observed significant changes in the secondary structure of bovine serum albumin (BSA) after glycation by ribose (RBSA). They indicated that an increase in β-sheet content in RBSA is pivotal for protein aggregation [37]. On the other hand, some authors have proposed that glycation may induce aggregation not by unfolding but through overall stabilization of the macromolecule, enhancing protein stability and prolonging its lifespan [38].

The formation of LOS-albumin complexes did not substantially impact the wavelength at which the spectrum reaches its minimum or the mean residue ellipticity values (Table 6). As demonstrated in Table 7, the binding of LOS to HSA and gHSA$_{GLC}$ did not lead to significant alterations in the macromolecule's secondary structure beyond 2%. Similarly, as in this work, Żurawska-Płaksej et al. observed only slight changes in the secondary structure of non-glycated and glycated BSA upon binding with gliclazide (GLICL). The authors emphasized that the decrease in α-helix content indicates a certain degree of structural unfolding, suggesting that GLICL is a weak modifier of BSA's

 doi:10.20944/preprints202408.0250.v1

secondary structure [39]. However, in the presented study, the α-helix content of gHSA$_{FRC}$ increased from 20% to 29.9% upon interaction with LOS (Table 7). This result may indicate that LOS stabilizes the secondary structure of the glycated by fructose protein. This stabilization could result from forming new hydrogen bonds or other interactions between the ligand and albumin, leading to more significant structural organization and increased α-helix content. Based on the DSSP (Dictionary of Secondary Structure of Proteins) method, Moeinpour et al. observed that LOS subtly impacts hydrogen bonds and, consequently, the secondary structure of HSA [40]. It should be emphasized that studies using CD spectroscopy to investigate the secondary structure of proteins after glycation are inconclusive. Some researchers have noted glucose concentration-dependent changes in CD spectra, while others have observed partial denaturation and structural disintegration [41]. The results presented in this study indicate that various sugars, as glycation inducers, can affect the secondary structure of human serum albumin differently.

3. Materials and Methods

3.1. Chemicals and Reagents

ImmunO Human serum albumin, fraction V, was purchased from MP Biomedicals LLC (Illkirch, France) and used without further purification; glipizide (GLP), losartan (LOS), sodium azide (NaN_3) and dimethyl sulfoxide (DMSO) were provided by Sigma-Aldrich Chemical Co. (Darmstadt, Germany); D(-)-fructose (FRC), D(+)-glucose (GLC) were obtained from POCH S.A. (Gliwice, Poland); di-Potassium hydrogen phosphate pure p.a. (K_2HPO_4) and sodium dihydrogen phosphate dehydrate ($NaH_2PO_4 \times 2H_2O$) were from Eurochem BGD Sp. z o.o. (Tarnów, Poland). All chemicals and reagents were of the highest analytical grade.

3.2. Methods

3.2.1. Sample Preparation

HSA Glycation: Before the in vitro glycation of human serum albumin (HSA), all glassware and spatulas were sterilized to prevent bacterial contamination. Glycated albumins (gHSA$_{GLC}$ and gHSA$_{FRC}$) were prepared by exposing HSA solutions (5×10^{-6} mol·L^{-1}) to D(+)-glucose (GLC) (0.05 mol·L^{-1}) and D(-)-fructose (FRC) (0.05 mol·L^{-1}) in a phosphate buffer (0.05 mol·L^{-1}) preserved with sodium azide (0.015 mol·L^{-1}) for 21 days incubation at a temperature of t = 37°C. A control sample (HSA) was prepared in the same manner but without the addition of reducing sugars. After the incubation period, the non-glycated HSA and glycated albumins were extensively dialyzed against phosphate buffer (pH = 7.4 ± 0.1) for 24 hours to remove the excess unbound GLC and FRC, then passed through a sterile Millex-GP syringe filter with 0.2 µm pores. The pH of the buffer solution, HSA, gHSA$_{GLC}$ and gHSA$_{FRC}$ was confirmed using a pH meter (FEP20 Mettler Toledo, Columbus, Ohio, USA). The absorbance ratio of HSA, gHSA$_{GLC}$ and gHSA$_{FRC}$ at λ = 255 nm and λ = 280 nm was less than 0.5, indicating the purity of the prepared albumin solutions.

Investigating the Interaction of Losartan (LOS) and Glipizide (GLP) with Non-glycated and Glycated Human Serum Albumins in Binary and Ternary Complexes: A quantitative analysis of the competition between LOS and GLP for the binding site in HSA, gHSA$_{GLC}$ and gHSA$_{FRC}$ was conducted using fluorimetric titration. To obtain the binary complexes of LOS and GLP with non-glycated and glycated albumins (LOS-HSA, LOS-gHSA$_{GLC}$, LOS-gHSA$_{FRC}$, and GLP-HSA, GLP-gHSA$_{GLC}$, GLP-gHSA$_{FRC}$), the albumin solutions (5×10^{-6} mol·L^{-1}) were titrated directly in the cuvette by adding increasing aliquots of LOS (5×10^{-3} mol·L^{-1}) and GLP (2.5×10^{-3} mol·L^{-1}) using a Hamilton syringe. The concentration range for LOS was from 5×10^{-6} mol·L^{-1} to 5×10^{-5} mol·L^{-1}, and for GLP, it was from 2.5×10^{-6} mol·L^{-1} to 2.5×10^{-5} mol·L^{-1}. To obtain the ternary complexes LOS-HSA-GLP$_{const}$, LOS-gHSA$_{GLC}$-GLP$_{const}$, LOS-gHSA$_{FRC}$-GLP$_{const}$, GLP-HSA-LOS$_{const}$, GLP-gHSA$_{GLC}$-LOS$_{const}$, and GLP-gHSA$_{FRC}$-LOS$_{const}$, the albumin solution (5×10^{-6} mol·L^{-1}) in the presence of GLP (5×10^{-6} mol·L^{-1}) or LOS (5×10^{-6} mol·L^{-1}) (molar ratio drug:albumin 1:1) was titrated in the cuvette by adding ten aliquots of LOS (5×10^{-3} mol·L^{-1}) or GLP (2.5×10^{-3} mol·L^{-1}), respectively. This procedure was conducted

 doi:10.20944/preprints202408.0250.v1

directly before fluorescence measurements. The LOS and GLP stock solutions were meticulously prepared by dissolving the appropriate amounts in distilled water and DMSO (ensuring DMSO did not exceed 1% *v/v* in the final concentration), respectively.

Investigating Ligand Interactions–Spectrophotometric Analysis of LOS and GLP: The solutions of LOS and GLP at a concentration of 2.5 × 10^{-5} mol·L^{-1}, as well as the drug mixture (GLP+LOS; GLP:LOS molar ratio 1:1), were prepared in phosphate buffer (pH = 7.4 ± 0.1, 0.05 mol·L^{-1}), by diluting the stock solutions of the drugs (2.5 × 10^{-3} mol·L^{-1}).

Spectropolarimetric Analysis of Glycation and LOS Influence on Macromolecule Secondary Structure: In this study, the samples (HSA, gHSA$_{GLC}$, and gHSA$_{FRC}$ at a concentration of 5 × 10^{-6} mol·L^{-1} each, as well as the LOS-HSA, LOS-gHSA$_{GLC}$, LOS-gHSA$_{FRC}$ complexes, where the molar ratio of LOS to albumin was 10:1) were prepared according to the procedure described above.

3.2.2. Fluorescence, UV-Vis and Dichroism (CD) Spectra Measurements

The samples' fluorescence spectra were measured at t = 37°C using a JASCO FP-6500 spectrofluorimeter (Hachioji, Tokyo, Japan) equipped with a Peltier thermostat and standard quartz cells. Excitation at λ_{ex} = 335 nm (λ_{em} = 350–500 nm) and λ_{ex} = 485 nm (λ_{em} = 500–580 nm) was used to measure the fluorescence of Advanced Glycation End-products (AGEs) in non-glycated (HSA) and glycated human serum albumin (gHSA$_{GLC}$, gHSA$_{FRC}$).

To excite the albumin fluorophores (Tyr and Trp-214 residues) in the binary (LOS-HSA, LOS-gHSA$_{GLC}$, LOS-gHSA$_{FRC}$, GLP-HSA, GLP-gHSA$_{GLC}$, GLP-gHSA$_{FRC}$) and ternary systems (LOS-HSA-GLP$_{const}$, LOS-gHSA$_{GLC}$-GLP$_{const}$, LOS-gHSA$_{FRC}$-GLP$_{const}$, GLP-HSA-LOS$_{const}$, GLP-gHSA$_{GLC}$-LOS$_{const}$, and GLP-gHSA$_{FRC}$-LOS$_{const}$), excitation wavelengths of λ_{ex} = 275 nm (excites Tyr and Trp-214 residues, λ_{em} = 285–400 nm) and λ_{ex} = 295 nm (excites Trp-214 residue, λ_{em} = 305–400 nm) were used. Finally, using JASCO software (Spectra Manager), the light scattering spectrum of the buffer was subtracted from all fluorescence spectra.

Due to the inner filter effect resulting from the presence of the drugs, the recorded fluorescence of HSA, gHSA$_{GLC}$, gHSA$_{FRC}$ in the binary and ternary systems was corrected using Equation (1) [42]:

$$F_{cor} = F_{obs} \cdot e^{\left(\frac{Abs_{ex}+Abs_{em}}{2}\right)} \qquad (1)$$

where: F_{cor} and F_{obs} are the corrected and observed fluorescence intensities, respectively; and Abs_{ex} and Abs_{em} are the absorbance at the excitation and emission wavelengths, respectively.

The samples' absorbance measurements were recorded using a model V-760 JASCO spectrophotometer (Easton, Maryland, USA) equipped with a thermostat bath, using quartz cuvettes of dimensions 1.0 cm × 1.0 cm × 4.0 cm. The apparatus has a wavelength correction error of ± 0.3 nm and a photometric correction error of ± 0.002 Abs at 0.5 Abs.

The absorption spectra of GLP and LOS at a concentration of 2.5 × 10^{-5} mol·L^{-1}, as well as the GLP+LOS system at GLP:LOS 1:1 (*v/v*) molar ratio, were determined in the wavelength range of λ = 235–300 nm at t = 37°C.

Far-UV CD spectra of HSA, gHSA$_{GLC}$, gHSA$_{FRC}$ and LOS-HSA, LOS-gHSA$_{GLC}$, and LOS-gHSA$_{FRC}$ complexes were recorded using a JASCO model J-1500 CD spectropolarimeter (Hachioji, Tokyo, Japan) equipped with a thermostatic Peltier cell holder (accuracy t = ± 0.05°C). All spectra were measured in a 0.1 cm path length quartz cuvette and scanned from λ = 200–250 nm at wavelength intervals of 0.2 nm, with a bandwidth set at 2.0 nm and D.I.T. of 4 seconds. CD intensity is expressed as mean residue ellipticity at wavelength λ ($[\theta]_{mrw}$) (deg·cm^2·$dmol^{-1}$) according to Equation (2) [36]:

$$[\theta]_{mrw} = \frac{MRW \cdot \theta_\lambda}{10 \cdot d \cdot c} \qquad (2)$$

where: MRW is the Mean Residue Weight (MRW_{HSA} = 113.7 Da); θ_λ is the observed ellipticity at wavelength λ (deg); d is the optical path–length (cm); c is the protein concentration (g·cm^{-3}).

The content of the samples' secondary structure elements was calculated using the Secondary Structure Estimation program with Yang's Reference model.

The fluorescence, absorption, and Far-UV CD spectra presented in this study were corrected by smoothing using the Savitzky and Golay method with a convolution width of 15, using the Spectra Analysis program (version 1.53.07, JASCO, Easton, Maryland, USA). Linear regression was

 doi:10.20944/preprints202408.0250.v1

performed by fitting the experimental data to the corresponding equation using Origin version 8.5 software (Northampton, MA, USA).

Based on the calculated fluorescence emission intensities, the quenching curves ($\frac{F}{F_0}$ vs. drug:albumin molar ratio, where: F, F_0 are the fluorescence intensities in the presence and absence of the quencher, respectively) of non-glycated and glycated human serum albumin in the presence of losartan (LOS) or glipizide (GLP) (binary system: LOS-HSA, LOS-gHSA$_{GLC}$, LOS-gHSA$_{FRC}$ and GLP-HSA, GLP-gHSA$_{GLC}$, GLP-gHSA$_{FRC}$) or in the presence of both drugs (ternary system: LOS-HSA-GLP$_{const}$, LOS-gHSA$_{GLC}$-GLP$_{const}$, LOS-gHSA$_{FRC}$-GLP$_{const}$ and GLP-HSA-LOS$_{const}$, GLP-gHSA$_{GLC}$-LOS$_{const}$, GLP-gHSA$_{FRC}$-LOS$_{const}$) were plotted.

The fluorescence quenching mechanism of HSA, gHSA$_{GLC}$ and gHSA$_{FRC}$ in the absence or presence of LOS and GLP in the binary and ternary systems was analyzed based on the Stern-Volmer equation (Equation (3)) [27]:

$$\frac{F_0}{F} = 1 + k_q\tau_0 \cdot [Q] = 1 + K_{SV} \cdot [Q] \quad (3)$$

where: k_q is the bimolecular quenching rate constant (L·mol^{-1}·s^{-1}), $k_q = \frac{K_{SV}}{\tau_0}$; τ_0 is the average fluorescence lifetime of albumin without a quencher, $\tau_0 = 6.0 \times 10^{-9}$ s [26]; K_{SV} is the Stern-Volmer constant (L·mol^{-1}); $[Q]$ is the concentration of the quencher (mol·L^{-1}).

The association constant (K_a) and the number of binding sites classes (n) in the ligand-albumin or ligand-albumin-ligand$_{const}$ complexes were determined using the Scatchard (Equation (4)) [43] and Klotz (Equation (5)) equations [44]:

$$\frac{r}{[L_f]} = n \cdot K_a - K_a \cdot r \quad (4)$$

$$\frac{1}{r} = \frac{1}{n} + \frac{1}{n \cdot K_a \cdot [L_f]} \quad (5)$$

where: $r = \frac{[L_b]}{[P]}$ is the number of ligand moles bound to one mole of protein; $[L_b]$ and $[L_f]$ are the bound and unbound drug concentrations, respectively and $[P]$ is the total protein concentration (mol·L^{-1}).

For two classes of binding sites in albumin structure (in this study GLP-HSA and LOS-gHSA$_{FRC}$-GLP$_{const}$ complexes), the binding isotherms were drawn using non-linear regression analysis according to Equation (6) and the association constants (K_{a1}, K_{a2}) and the number of binding sites (n_1, n_2) were calculated [45]:

$$r = \frac{n_1 \cdot K_{a1} \cdot [L_f]}{1 + K_{a1} \cdot [L_f]} + \frac{n_2 \cdot K_{a2} \cdot [L_f]}{1 + K_{a2} \cdot [L_f]} \quad (6)$$

Hill's coefficient n_H was determined on the basis of the Hill method (Equation (6)) [46]:

$$\log\left(\frac{r}{1-r}\right) = n_H \cdot \log[L_f] + \log K_a \quad (7)$$

4. Conclusions

The main goal of this project was to analyze the interactions of losartan (LOS) and glipizide (GLP) with non-glycated (HSA) and glycated human serum albumin (gHSA$_{GLC}$ and gHSA$_{FRC}$) and to investigate their mutual competition in the binding sites of the macromolecule using multiple spectroscopic techniques.

The analysis of the emission fluorescence spectra of glycation products (AGEs) indicated that fructose (FRC) is a more effective glycation agent for HSA than glucose (GLC). This conclusion is supported by the observation that glycation in the presence of FRC leads to a faster and more efficient Amadori rearrangement. Glycation induces conformational changes in the albumin structure, particularly altering the microenvironment around crucial amino acid residues (Trp-214 and Tyr), thus influencing their accessibility to quenchers. The results showed that LOS and GLP have a higher affinity for non-glycated HSA than glycated gHSA$_{GLC}$ and gHSA$_{FRC}$, forming a more stable complex.

 doi:10.20944/preprints202408.0250.v1

Additionally, LOS and GLP were found to interact nonspecifically with the hydrophobic fragments of the surface of albumins in binary (ligand-albumin) and ternary systems (ligand-albumin-ligand$_{const}$) and specifically saturate the binding sites within the protein molecule. An additional drug (GLP in the LOS-albumin complex or LOS in the GLP-albumin complex) complicates the interaction, likely leading to competitive binding or displacement of the initially bound drug in both non- and glycated albumins. Analysis of the CD spectra revealed that GLP and LOS interact with each other. This finding emphasizes the importance of closely monitoring patients' co-administered these drugs, focusing on blood glucose levels, blood pressure, and renal function to ensure safe and effective therapy.

In conclusion, the significant impact of glycation on the drug-binding capacity of albumin, as revealed by this study, has profound implications for patient care. Particularly for diabetic patients, the altered binding properties of glycated albumin could potentially compromise the efficacy and safety of drug therapy. Therefore, the need for careful monitoring and potentially adjusted dosing regimens is urgent to ensure optimal therapeutic outcomes. Further clinical studies are imperative to develop comprehensive guidelines for the concurrent use of LOS and GLP in polypharmacotherapy.

Supplementary Materials: The following supporting information can be downloaded at: Preprints.org, Figure S1: Quenching fluorescence of albumin non-glycated (HSA, ♦) and glycated (gHSA$_{GLC}$, ◊; gHSA$_{FRC}$, ♦) containing 5×10^{-6} mol·L^{-1} to 5×10^{-5} mol·L^{-1} concentrations of LOS (**a**, **b**) and 2.5×10^{-6} mol·L^{-1} to 2.5×10^{-5} mol·L^{-1} concentrations of GLP (**c**, **d**). Albumin concentration: 5×10^{-6} mol·L^{-1}; λ_{ex} = 275 nm (**a**, **c**) and λ_{ex} = 295 nm (**b**, **d**); error bars are smaller than the symbols; Figure S2: The Stern-Volmer curves for the binary (**a**) LOS-HSA, LOS-gHSA$_{GLC}$, LOS-gHSA$_{FRC}$; (**b**) GLP-HSA, GLP-gHSA$_{GLC}$, GLP-gHSA$_{FRC}$ and ternary systems (**c**) LOS-HSA-GLP$_{const}$, LOS-gHSA$_{GLC}$-GLP$_{const}$, LOS-gHSA$_{FRC}$-GLP$_{const}$; (**d**) GLP-HSA-LOS$_{const}$, GLP-gHSA$_{GLC}$-LOS$_{const}$, GLP-gHSA$_{FRC}$-LOS$_{const}$; λ_{ex} = 295 nm; error bars are smaller than the symbols used in the plots; Figure S3: Binding isotherms of HSA, gHSA$_{GLC}$ and gHSA$_{FRC}$ at 5×10^{-6} mol·L^{-1} concentration with LOS at 5×10^{-6} mol·L^{-1} to 5×10^{-5} mol·L^{-1} and GLP at 2.5×10^{-6} mol·L^{-1} to 2.5×10^{-5} mol·L^{-1} concentrations in the binary (**a**) LOS-HSA, LOS-gHSA$_{GLC}$, LOS-gHSA$_{FRC}$; (**b**) GLP-HSA, GLP-gHSA$_{GLC}$, GLP-gHSA$_{FRC}$ and ternary systems (**c**) LOS-HSA-GLP$_{const}$, LOS-gHSA$_{GLC}$-GLP$_{const}$, LOS-gHSA$_{FRC}$-GLP$_{const}$; with GLP at 5×10^{-6} mol·L^{-1} concentration, (**d**) GLP-HSA-LOS$_{const}$, GLP-gHSA$_{GLC}$-LOS$_{const}$, GLP-gHSA$_{FRC}$-LOS$_{const}$ with LOS at 5×10^{-6} mol·L^{-1} concentration, λ_{ex} = 295 nm; error bars are smaller than the symbols used in the plots; Figure S4: Scatchard plots for the binary (**a**) LOS-HSA, LOS-gHSA$_{GLC}$, LOS-gHSA$_{FRC}$; (**b**) GLP-HSA, GLP-gHSA$_{GLC}$, GLP-gHSA$_{FRC}$ and ternary systems (**c**) LOS-HSA-GLP$_{const}$, LOS-gHSA$_{GLC}$-GLP$_{const}$, LOS-gHSA$_{FRC}$-GLP$_{const}$; (**d**) GLP-HSA-LOS$_{const}$, GLP-gHSA$_{GLC}$-LOS$_{const}$, GLP-gHSA$_{FRC}$-LOS$_{const}$; λ_{ex} = 295 nm; error bars are smaller than the symbols used in the plots; Figure S5: Klotz curves for the binary (**a**) LOS-HSA, LOS-gHSA$_{GLC}$, LOS-gHSA$_{FRC}$; (**b**) GLP-HSA, GLP-gHSA$_{GLC}$, GLP-gHSA$_{FRC}$ and ternary systems (**c**) LOS-HSA-GLP$_{const}$, LOS-gHSA$_{GLC}$-GLP$_{const}$, LOS-gHSA$_{FRC}$-GLP$_{const}$; (**d**) GLP-HSA-LOS$_{const}$, GLP-gHSA$_{GLC}$-LOS$_{const}$, GLP-gHSA$_{FRC}$-LOS$_{const}$; λ_{ex} = 295 nm; error bars are smaller than the symbols used in the plots; Figure S6: Hill plots for the binary (**a**) LOS-HSA, LOS-gHSA$_{GLC}$, LOS-gHSA$_{FRC}$; (**b**) GLP-HSA, GLP-gHSA$_{GLC}$, GLP-gHSA$_{FRC}$ and ternary systems (**c**) LOS-HSA-GLP$_{const}$, LOS-gHSA$_{GLC}$-GLP$_{const}$, LOS-gHSA$_{FRC}$-GLP$_{const}$; (**d**) GLP-HSA-LOS$_{const}$, GLP-gHSA$_{GLC}$-LOS$_{const}$, GLP-gHSA$_{FRC}$-LOS$_{const}$; λ_{ex} = 295 nm; error bars are smaller than the symbols used in the plots; Table S1: The percentage (%) of fluorescence quenching of non-glycated (HSA) and glycated albumin (gHSA$_{GLC}$, gHSA$_{FRC}$) in the presence of losartan (LOS) and glipizide (GLP) with increasing concentration; λ_{ex} = 275 nm and λ_{ex} = 295 nm.

Author Contributions: Conceptualization, A.S.; methodology, A.S.; software, A.S.; validation, A.S.; formal analysis, A.S.; investigation, A.S.; resources, A.S.; data curation, A.S.; writing—original draft preparation, A.S.; writing—review and editing, A.S.; visualization, A.S.; supervision, A.S.; project administration, A.S.; funding acquisition, A.S. The author has read and agreed to the published version of the manuscript.

Funding: This research was funded by the Medical University of Silesia, Katowice, Poland (Grant No. PCN-2-012/K/1/F and PCN-2-013/K/2/F).

Institutional Review Board Statement: Not applicable.

Informed Consent Statement: Not applicable.

Data Availability Statement: The data underlying the findings of this study are accessible upon reasonable request to the author.

Conflicts of Interest: The author declares no conflicts of interest. The funders had no role in the design of the study; in the collection, analyses, or interpretation of data; in the writing of the manuscript; or in the decision to publish the results.

References

1. Ghosh, R.; Kishore N. Mechanistic physicochemical insights into glycation and drug binding by serum albumin: Implications in diabetic conditions. *Biochimie* **2022**, *193*, 16–37. https://doi.org/10.1016/j.biochi.2021.10.008
2. Neelofar, K.M.; Arif, Z.; Alam, K.; Ahmad J. Hyperglycemia induced structural and functional changes in human serum albumin of diabetic patients: a physico-chemical study. *Mol. BioSyst.* **2016**, *12*(8), 2481–2489. http://dx.doi.org/10.1039/C6MB00324A
3. Manolis, A.A.; Manolis, T.A.; Melita, H.; Mikhailidis, D.P.; Manolis, A.S. Low serum albumin: A neglected predictor in patients with cardiovascular disease. *Eur. J. Intern. Med.* **2022**, *102*, 24–39. https://doi.org/10.1016/j.ejim.2022.05.004
4. Rabbani, N.; Tabrez, S.; Islam, B.U.; Rehman, M.T.; Alsenaidy, A.M.; AlAjmi, M.F.; Khan, R.A.; Alsenaidy, M.A.; Khan, M.S. Characterization of colchicine binding with normal and glycated albumin: In vitro and molecular docking analysis. *J. Biomol. Struct. Dyn.* **2018**, *36*(13), 3453–3462. https://doi.org/10.1080/07391102.2017.1389661
5. Whelton, P.K.; He, J.; Oparil, S.; Wright, J.T.; Appel, L.J.; Cutler, J.A.; Havas, S.; Kotchen, T.A.; Roccella, E.J.; Karimbakas, J. Effects of oral losartan on blood pressure and risk of adverse cardiovascular outcomes in hypertensive patients with left ventricular hypertrophy: A randomized controlled trial. *The Lancet* **2002**, *359*(9312), 995–1003. https://doi.org/10.1016/S0140-6736(02)08020-3
6. Al-Majed, A.R.; Assiri, E.; Khalil, N.Y.; Abdel-Aziz, H.A. Losartan: Comprehensive Profile. *Profiles Drug. Subst. Excip. Relat. Methodol.* **2015**, *40*, 159–194. https://doi.org/10.1016/bs.podrm.2015.01.002
7. Sica D.A.; Gehr T.W.; Ghosh S. Clinical pharmacokinetics of losartan. *Clin. Pharmacokinet.* **2005**, *44*, 797–814. http://doi.org/10.2165/00003088-200544080-00003
8. Anwer, R.; AlQumaizi, K.I.; Haque, S.; Somvanshi, P.; Ahmad, N.; AlOsaimi, S.M.; Fatma, T. Unravelling the interaction of glipizide with human serum albumin using various spectroscopic techniques and molecular dynamics studies. *J. Biomol. Struct. Dyn.* **2021**, *39*(1), 336–347. https://doi.org/10.1080/07391102.2019.1711195
9. Matsuda, R.; Li, Z.; Zheng, X.; Hage, D.S. Analysis of glipizide binding to normal and glycated human serum albumin by high-performance affinity chromatography. *Anal. Bioanal. Chem.* **2015**, *407*(18), 5309–5321. https://doi.org/10.1007/s00216-015-8688-0
10. Siligardi, G.; Hussain, R.; Patching, S.G.; Phillips-Jones, M.K. Ligand- and drug-binding studies of membrane proteins revealed through circular dichroism spectroscopy. *Biochim. Biophys. Acta* **2014**, *1838*, 34–42. https://doi.org/10.1016/j.bbamem.2013.06.019
11. Szkudlarek, A.; Pentak, D.; Ploch, A.; Pożycka, J.; Maciążek-Jurczyk, M. In Vitro Investigation of the Interaction of Tolbutamide and Losartan with Human Serum Albumin in Hyperglycemia States. *Molecules* **2017**, *22*(12), 2249. https://doi.org/10.3390/molecules22122249
12. Szkudlarek, A. Effect of Palmitic Acid on Tertiary Structure of Glycated Human Serum Albumin. *Processes* **2023**, *11*, 2746. https://doi.org/10.3390/pr11092746
13. Maciążek-Jurczyk, M.; Szkudlarek, A.; Chudzik, M.; Pożycka, J.; Sułkowska, A. Alteration of human serum albumin binding properties induced by modifications: A review. *Spectrochim. Acta Part A Mol. Biomol. Spectrosc.* **2017**, *188*, 675–683. http://doi.org/10.1016/j.saa.2017.05.023
14. Johnson, R.J.; Segal, M.S.; Sautin, Y.; Nakagawa, T.; Feig, D.I.; Kang, D.H.; Gersch, M.S.; Benner, S.; Sánchez-Lozada, L.G. Potential role of sugar (fructose) in the epidemic of hypertension, obesity and the metabolic syndrome, diabetes, kidney disease, and cardiovascular disease. *Am. J. Clin. Nutr.* **2007**, *86*(4), 899–906. https://doi.org/10.1093/ajcn/86.4.899
15. Bjornstad, P.; Lanaspa, M.A.; Ishimoto, T.; Kosugi, T.; Kume, S.; Jalal, D.; Maahs, D.M.; Snell-Bergeon, J.K.; Johnson, R.J.; Nakagawa, T. Fructose and uric acid in diabetic nephropathy. *Diabetologia* **2015**, *58*(9), 1993–2002. https://doi.org/10.1007/s00125-015-3650-4
16. Padayatti, P.S.; Ng, A.S.; Uchida, K.; Glomb, M.A.; Nagaraj, R.H. Argpyrimidine, a blue fluorophore in human lens proteins: high levels in brunescent cataractous lenses. *Invest. Ophthalmol. Vis. Sci.* **2001**, *42*(6), 1299–1304.
17. Kessel, L.; Kalinin, S.; Nagaraj, R.H.; Larsen, M.; Johansson, L.B. Time-resolved and steady-state fluorescence spectroscopic studies of the human lens with comparison to argpyrimidine, pentosidine and 3-OH-kynurenine. *Photochem. Photobiol* **2002**, *76*(5), 549–554. https://doi.org/10.1562/0031-8655(2002)076<0549:trassf>2.0.co;2
18. Schmitt, A.; Schmitt, J.; Münch, G.; Gasic-Milencovic, J. Characterization of advanced glycation end products for biochemical studies: side chain modifications and fluorescence characteristics. *Anal.*

Biochem. **2005**, *338*(2), 201–215. https://doi.org/10.1016/j.ab.2004.12.003
19. Starosta, R.; Santos, F.C.; Almeida, R.D. Human and bovine serum albumin time-resolved fluorescence: Tryptophan and tyrosine contributions, effect of DMSO and rotational diffusion. *J. Mol. Struct.* ***2020***, *1221*, 128805. https://doi.org/10.1016/j.molstruc.2020.128805
20. Obara, S.; Nakane, K.; Fujimura, C.; Tomoshige, S.; Ishikawa, M.; Sato, S. Functionalization of Human Serum Albumin by Tyrosine Click. *Int. J. Mol. Sci.* **2021**, *22*, 8676. https://doi.org/10.3390/ijms22168676
21. Valeur, B. *Molecular Fluorescence: Principles and Applications*; Wiley-VCH: London, UK; Weinheim, Germany, 2002.
22. Sudlow, G.; Birkett, D.J.; Wade, D.N. The characterization of two specific drug binding sites on human serum albumin. *Mol. Pharmacol.* **1975**, *11*(6), 824–832.
23. Stryer L. Fluorescence spectroscopy of proteins. *Science* **1978**, *162*, 526–533.
24. Iberg, N.; Flückiger, R. Nonenzymatic glycosylation of albumin in vivo. Identification of multiple glycosylated sites. *J. Biol. Chem.* **1986**, *261*(29), 13542–13545.
25. Eftink, M.R.; Ghiron, C.A. Fluorescence quenching studies with proteins. *Anal. Biochem.* **1981**, *114*(2), 199–227. https://doi.org/10.1016/0003-2697(81)90474-7
26. Lakowicz, J.R.; Weber, G. Quenching of protein fluorescence by oxygen. Detection of structural fluctuations in proteins on the nanosecond time scale. *Biochemistry*, **1973**, *12*(21), 4171–4179. https://doi.org/10.1021/bi00745a021
27. Lakowicz, J.R. *Principles of Fluorescence Spectroscopy*, 3rd ed.; Springer: New York, NY, USA, 2006; pp.1–535.
28. Gehlen, M.H. The centenary of the Stern-Volmer equation of fluorescence quenching: From the single line plot to the SV quenching map. *J. Photochem. Photobiol. C Photochem. Rev.* **2020**, *42*, 100338. https://doi.org/10.1016/j.jphotochemrev.2019.100338
29. Taira, Z.; Terada, H. Specific and non-specific ligand binding to serum albumin. *Biochem. Pharmacol.* **1985**, *34*(11), 1999–2005. https://doi.org/10.1016/0006-2952(85)90322-3
30. Koyama, H.; Sugioka, N.; Uno, A.; Mori, S.; Nakajima, K. Effects of glycosylation of hypoglycaemic drug binding to serum albumin. *Biopharm. Drug Dispos.* **1997**, *18*(9), 791–801. https://doi.org/10.1002/(sici)1099-081x(199712)18:9<791::aid-bdd66>3.0.co;2-1
31. Wiglusz, K.; Żurawska-Płaksej, E.; Rorbach-Dolata, A.; Piwowar, A. How Does Glycation Affect Binding Parameters of the Albumin-Gliclazide System in the Presence of Drugs Commonly Used in Diabetes? In Vitro Spectroscopic Study. *Molecules* **2021**, *26*(13), 3869. https://doi.org/10.3390/molecules26133869
32. Chume, F.C.; Kieling, M.H.; Correa Freitas, P.A.; Cavagnolli, G.; Camargo, J.L. Glycated albumin as a diagnostic tool in diabetes: An alternative or an additional test? *PloS One* **2019**, *14*(12), e0227065. https://doi.org/10.1371/journal.pone.0227065
33. Goutelle, S.; Maurin, M.; Rougier, F.; Barbaut, X.; Bourguignon, L.; Ducher, M.; Maire, P. The Hill equation: a review of its capabilities in pharmacological modelling. *Fundam. Clin. Pharmacol.* **2008**, *22*(6), 633–648. https://doi.org/10.1111/j.1472-8206.2008.00633.x
34. Ren, G.; Sun, H.; Guo, J.; Fan, J.; Li, G.; Xu, S. Molecular mechanism of the interaction between resveratrol and trypsin via spectroscopy and molecular docking. *Food Funct.* **2019**, *10*, 3291–3302. https://doi.org/10.1039/c9fo00183b
35. Pelton, J.T.; McLean, L.R. Spectroscopic Methods for Analysis of Protein Secondary Structure. *Anal. Biochem.* **2000**, *277*, 167–176. https://doi.org/10.1006/abio.1999.4320
36. Kelly, S.M.; Jess, T.J.; Price, N.C. How to study proteins by circular dichroism. *Biochim. Biophys. Acta* **2005**, *1751*, 119–139. https://doi.org/10.1016/j.bbapap.2005.06.005
37. Mou, L.; Hu, P.; Cao, X.; Chen, Y.; Xu, Y.; He, T.; Wei, Y.; He, R. Comparison of bovine serum albumin glycation by ribose and fructose in vitro and in vivo. *Biochim. Biophys. Acta (BBA) - Mol. Basis Dis.* **2022**, *1868*, 166283. https://doi.org/10.1016/j.bbadis.2021.166283
38. Rondeau, P.; Bourdon, E. The glycation of albumin: Structural and functional impacts, *Biochimie*, **2011**, *93*, 645–658. https://doi.org/10.1016/j.biochi.2010.12.003
39. Żurawska-Płaksej, E.; Rorbach-Dolata, A.; Wiglusz, K; Piwowar, A. The effect of glycation on bovine serum albumin conformation and ligand binding properties with regard to gliclazide. *Spectrochim. Acta A Mol. Biomol. Spectrosc.*, **2018**, 189, 625–633. https://doi.org/10.1016/j.saa.2017.08.071
40. Moeinpour, F.; Mohseni-Shahri, F.S.; Malaekeh-Nikouei, B.; Nassirli, H. Investigation into the interaction of losartan with human serum albumin and glycated human serum albumin by spectroscopic and molecular dynamics simulation techniques: A comparison study. *Chem. Biol. Interact.* **2016**, *257*, 4–13. https://doi.org/10.1016/j.cbi.2016.07.025
41. Monacelli, F.; Storace, D.; D'Arrigo, C.; Sanguineti, R.; Borghi, R.; Pacini, D.; Furfaro, A.L.; Pronzato, M.A.; Odetti, P.; Traverso, N. Structural Alterations of Human Serum Albumin Caused by Glycative and Oxidative Stressors Revealed by Circular Dichroism Analysis. *Int. J. Mol. Sci.* **2013**, *14*, 10694–10709. https://doi.org/10.3390/ijms140610694

42. Kirby, E.P. Fluorescence Instrumentation and Methodology. In *Excited States of Proteins and Nucleic Acids*; Steiner, R.F., Weinryb, I., Eds.; Springer: Boston, MA, USA, 1971.
43. Scatchard, G. The attractions of proteins for small molecules and ions. *Ann. N Y Acad. Sci.* **1949**, *51*, 660–672. https://doi.org/10.1111/j.1749-6632.1949.tb27297.x
44. Klotz, I.M.; Hunston, D.L. Properties of graphical representations of multiple classes of binding sites. *Biochemistry* **1971**, *10*, 3065–3069. https://doi.org/10.1021/bi00792a013
45. Giesy, J.P.; Alberts, J.J. Conditional stability constans and binding capacities for copper (II) by ultrafilterable material isolated from six surface waters of Wyoing, USA: *Hydrobiologia* **1989**; *188*, 659–680. https://doi.org/10.1007/BF00027834
46. Goutelle, S.; Maurin, M.; Rougier, F.; Barbaut, X.; Bourguignon, L.; Ducher, M.; Maire, P. The Hill equation: a review of its capabilities in pharmacological modelling. *Fundam. Clin. Pharmacol*. **2008**, *22*(6), 633–648.
47. https://doi.org/10.1111/j.1472-8206.2008.00633.x